AN EXPERIMENTAL STUDY ON INCIPIENT CONDITION OF TOE PROTECTION ELEMENTS OF RIVER BANK PROTECTION WORKS

Md. Hamiduzzaman

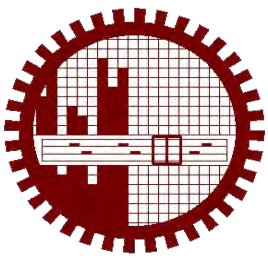

DEPARTMENT OF WATER RESOURCES ENGINEERING
BANGLADESH UNIVERSITY OF ENGINEERING AND TECHNOLOGY
(BUET), DHAKA-1000
MARCH, 2019

AN EXPERIMENTAL STUDY ON INCIPIENT CONDITION OF TOE PROTECTION ELEMENTS OF RIVER BANK PROTECTION WORKS

A Thesis Submitted

By

MD. HAMIDUZZAMAN

(0412162068)

A thesis submitted to the Department of Water Resources Engineering
in partial fulfillment of the requirements for the Degree of
Master of **Engineering (in Water Resources Engineering)**

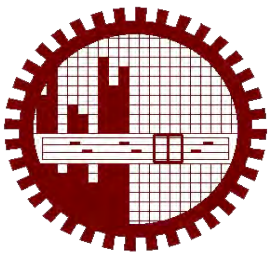

DEPARTMENT OF WATER RESOURCES ENGINEERING
BANGLADESH UNIVERSITY OF ENGINEERING AND TECHNOLOGY
(BUET), DHAKA-1000
MARCH, 2019

CERTIFICATION OF THESIS

The thesis titled **"An Experimental Study on Incipient Condition of Toe Protection Elements of River Bank Protection Works"**, submitted by Md. Hamidurzaman, Roll No. 0412162068, Session: April 2012, has been accepted as satisfactory in partial fulfillment of the requirements for the degree of **Master of Engineering in Water Resources Engineering** on 31st March, 2019.

Dr. K. M. Ahtesham Hossain — **Chairman (Supervisor)**
Assistant Professor
Department of Water Resources Engineering
BUET, Dhaka-1000, Bangladesh

Dr. Md. Abdul Matin — **Member**
Professor
Department of Water Resources Engineering,
BUET, Dhaka-1000, Bangladesh

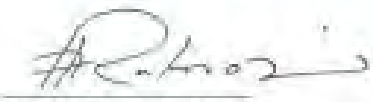

Dr. Md. Abdur Rahman — **Member**
Professor
Department of Water Resources Engineering,
BUET, Dhaka-1000, Bangladesh

MARCH, 2019

DECLARATION

This is to certify that this thesis work has been done by me and neither this thesis nor any part thereof has been submitted elsewhere for the award of any degree or diploma.

_____

Md.Hamiduzzaman

Signature of the Candidate

TABLEOFCONTENTS

Page No.

LISTOFFIGURES

LISTOFTABLES

LISTOFPHOTOGRAPHS

LISTOFNOTATIONS

A	Archimedes buoyancy index
a,b,c	Dimensionless numbers
C_2	Constant
C_S	Stability coefficient
C_T	Stability coefficient for incipient failure
C_T	Coefficient for riprap layer thickness
C_V	Coefficient for vertical velocity distribution
D	Depth of scour
D_n	Nominal thickness of protection unit
d	Characteristics diameter
d_n	Nominal diameter
d_l	Length of a particle
d_s	Mean sieve size of a particle
d_t	Thickness of a particle
d_w	Width of a particle
D_s	Scour depth
d_{30}	Particlesizeforwhich30%byweightisfiner
d_{50}	Medianparticlediameterforwhich50%byweightisfiner
d_9	Particlesizeforwhich90%byweightisfiner
F	Freeboard
f	Lacey's silt factor
X	Multiplying factor
g	Gravitational acceleration
h	Depth of flow
K	Empirical constant
k	Empirical coefficient
K_1	Side slope correction factor

K_h	Depth & velocity distribution factor
ρ_w	Water density
α	Slope angle
Q_c	Critical value of dimension less shear stress
Q	Design Discharge
k_S	Effective bed roughness
m	Empirical exponent
R	Lacey's regime scour depth
R^2	Coefficient of determination
R'	Rise of flood
R^*_C	Critical boundary Reynolds number
S_f	Safety factor
T	Thickness of slope stone
T_1	Thickness of stone on prospective slope below bottom of apron
U	Depth averaged horizontal velocity of element
u	Horizontal velocity of element
u_{oc}	Critical velocity near the bed
$\bar{u}_C$	Critical depth-averaged velocity
U^*_C	Critical friction velocity
V	Depth averaged flow velocity
W	Weight of a particle
γ	Unit weight of water
γ_S	Unit weight of particle
Δ	Relative submerged unit weight
ρ	Mass density of water
ρ_S	Mass density of particle
φ_c	Stability factor
τ_C	Critical shear stress
τ^*_C	Critical Shields stress
ν	Kinematic viscosity of water
K_T	Turbulent factor
$\forall$	Volume of original particle
ϕ	Slope of bed
θ	Angle of repose
U'	Turbulent fluctuation

LIST OF ABBREVIATIONS

BWDB	Bangladesh Water Development Board
CC Blocks	Cube shaped Concrete blocks
FAP	Flood Action Plan
PWD	Public Works Department
RRI	River Research Institute
DWL	Design Water Label
HWL	Highest Water Level
LWL	Lowest Water Level
RBPP	River Bank Protection Project
RWL	River Water Level

ACKNOWLEDGEMENT

At first, I would like to praise almighty Allah for his support in all aspect of my life. I wish to express profound gratitude and sincerest appreciation to my supervisor Dr. K. M. Ahtesham Hossain Assistant Professor Department of Water Resources Engineering, Bangladesh University of Engineering and Technology, Dhaka for inspiring me to conduct this thesis work and to provide me dexterous guide which help me to reach at culmination of the work successfully. The author is really grateful to the supervisor for his cordial supervision, intellectual guidance, valuable suggestions, constant support and encouragement at every stage of this study. Without coordination and help this study would have been incomplete.

I also would like to thank the assistants of Hydraulic Laboratory of BUET for their physical help to complete my laboratory experiment efficiently. The author is also indebted to the members of the examination committee Dr. Md. Abdul Matin, Professor Department of Water Resources Engineering, BUET, Dr. Md. Ataur Rahman,, Professor, Department of Water Resources Engineering, BUET.

I am also grateful to Dr. Md. Mostafa Ali, Professor and Head, Department of Water Resources Engineering, BUET, Dhaka, for providing all library facilities and laboratory facilities for accomplishing this study in a comprehensive manner.

The author is also thankful to lab assistant Mr. Shahjalal for providing the velocity measurement current meter during the experiments.

The author expresses profound thanks to him family members for supporting and inspiring to conduct the study. Above all, the author is grateful to the Almighty Allah who Has given him the opportunity to work hard.

Md. Hamiduzzaman

March, 2019.

ABSTRACT

The present study has been undertaken to investigate experimentally the incipient condition of to e protection elements. Relationships for governing parameters of the incipient velocity of toe protection elements have been theoretically analyzed. These relationships are then verified using laboratory data. The experiments are conducted in the large tilting flume of the Hydraulics and River Engineering Laboratory of Water Resources Engineering Department, BUET.A total of eighteen experimental run consisting of five different sizes (ranging from 20mm-24mm) of geobags and three different sizes (ranging from 16mm-23 mm) of CC blocks have been conducted in laboratory flume for discharges varying from 0.066 m^3/s to 0.187 m^3/s.During experimentation various observations are made and measured data are used to obtain relationships for the incipient condition of the toe protection elements.

An empirical relationship (equation 4.1) to determine the size of CC block as toe protection element based on incipient condition is developed with a coefficient of correlation (R^2) is 0.951. Also, an empirical relationship (equation 4.3) to determine the size of geobag as toe protection element based on incipient condition is developed with a coefficient of correlation (R^2) is 0.53.

Improved empirical relationship is found when both current and previous data are taken into account. For CC block, equation 4.5 ($R^2 = 0.854$), and for geobag, equation 4.6 ($R^2 = 0.321$), are proposed. For incipient condition, CC blocks can withstand at higher velocity at higher depths (Figure 4.8). Proposed relationships show indication to selection of larger protection unit than the conventional formula (Figure 4.9).

It is found from the study that for a given velocity the required thickness of protection decreases with the increase of depth of flow for CC block. However, reverse condition is observed for geobag (Figure 4.10). This discrepancy may be due to the fact that the geobags are relatively flat and less dense, and thus their underwater functional behavior becomes more composite as a group. Also, the specific gravity of geobag is almost half of the CC block.

Experimental results are analyzed to develop relationships between the relative size and flow parameters. Improved empirical relationship is found when both current and previous data are taken into account. Developed empirical relationships can be used to predict incipient condition for selected type and size of toe protection elements.

The proposed relationships are also compared with the equations available in previous studies. Proposed relationships show indication to selection of larger protection unit than the conventional formula.

It is hoped that the outcome of the present study can be used as a tentative guideline for design of toe protection elements in river bank protection works.

CHAPTER ONE

INTRODUCTION

1.1 Background of the Study

River bank erosion in major rivers has always been a difficult problem causing damage to valuable lands, settlements and infrastructures from year to year. Strong river currents erode the fine sand from the toe of the riverbank. To address this problem artificial covering of the riverbank and bed with erosion resistant material is constructed. Toe protection is required when water currents scour and undermine the toe of a bank resulting the sliding of slopes.

In revetment design procedures, now a days, cube shaped concrete block (CC block) with geosynthetic (geotextile) product have been increasingly used in erosion control and bank protection works (Figure 1). This protection element can be more cost effective if the readily available sand slurry is used in a container like geobags. In recent time, concrete blocks and geobags are commonly used as toe protection elements of revetment works.

Photograph 1.1: Sand filled geobag and cc block are used to protect river bank failure.

A cover of stone or cube shaped concrete block (cc block), known as an apron is laid on the toe of the bank of the river. An apron of toe protection is required to resist the undermining of bed resulting from scour in such a way that apron launches to cover the face with stone/cc block forming a continuous carpet below the permanent slope.

This apron of the toe protection is required to resist the undermining of the bed resulting from scour in such a way that apron launches to cover the face with stone forming a continuous carpet below the permanent slope. A sufficient quantity of stone for the apron has to be provided to ensure complete protection of the entire scoured face. The required quantity of stone should be placed in practice as accurately as possible. Strict supervision and quality control should be ensured. Further, number of study had been conducted for incipient condition of sediment particle. Examples are, works of Van Rijn (1993), Ünal and Bayazit (1998), Lick et al.(2004), Smith and Cheung (2004), Ling (1995), Beheshti and Ashtiani (2008), Marsh et al. (2004), Gogus and Defne (2005) and many others. Inglis (1949), Charles Neill (1967), Maynord (1987), USACE (1991), NHC (2006), Raju (2011), Ahmed (2014) proposed relationship regarding incipient motion of erosion resistant materials. Limited study had been done on incipient behavior of toe protection elements simulating the actual method of construction practiced in the field.

Identification of placement of protective elements in underwater flowing situation is found to be more difficult. This has been also reported by Stevens and Oberhagemann (2006). NHC (2006) advised more drop test to be conducted for a better insight. Stevens and Oberhagemann (2006) conducted research on rectangular shape and further recommended testing the behavior of square shaped geobag. Haque (2010) carried out an experimental investigation in a sand bed channel and observed the flow behavior around constructed apron for different flow conditions.

Ahmed (2014) conducted study on incipient condition of toe protection particles which is based on critical shear stress. Raju (2011) carried out investigation on incipient condition of toe protection elements of river bank protection works simulating the underwater construction/dumping process followed in the field. However, scope is still there to shed some more light. Because wider range of initial water flow depth in the tilting flume are yet to be conducted to achieve comprehensiveness of the study on incipient condition.

1.2 Objectives of the Study

The main objectives of the study have been setup as follows:

i) To investigate the threshold condition of different types of protective elements.

ii) To develop relationships for the estimation of incipient condition of the protective elements.

iii) Finally, to compare the available incipient velocity formulae with the proposed/developed formula based on experimental data.

1.3 Organization of the Thesis

This thesis has been organized under five chapters. **Chapter one** describes the background objectives and analysis of incipient motion of the study. In **Chapter two** the review of literature related to the subject matter of the study has been described. In **Chapter three,** theoretical background of experimentation is presented which is the basis of analysis of the experimental data. Analysis technique for incipient condition are stated. Illustrates the experimentation set-up of the laboratory, size of protection elements used, test scenarios, test procedures followed during measurements and the observations noted at that time. In **Chapter Four,** the results of analyses and discussions are presented. Finally, the main conclusions of this study and recommendations for further study are presented in **Chapter Five.**

CHAPTER TWO

LITERATURE REVIEW

2.1 Introduction

Sustainability of river bank protection works had been the subject of research for a long time. There are some modern and classical approaches available in literature for the design of bank protection works. Protection works mainly depends on its constructional aspects for design. The appropriate method of construction again depends on mechanism of incipient condition of protection element. In this chapter these hydraulic aspects of bank protection elements involved in the process are briefly reviewed.

2.2 River Bank Protection Works

River bank protection works are essentially important parts of river training works. The view point of bank protection structure is to design and construct structures to guide the water course at desired level allowing certain degree of damages which may be taken care of through monitoring and repair during occurrence of the extreme events. The purpose of these structures is to prevent bank erosion to provide a stable river bank. Some other functions of bank protection works are-

(a) Safe and expeditious passage of flood flow.

(b) Efficient transportation of suspended and bed loads.

(c) Stable river course with minimum bank.

(d) Sufficient depth and good course for navigation.

(e) Direction of flow through a certain defined stretch of the river, (Przedwojski et al., 1995).

The various kinds of protective works can be broadly classified into two groups, this being-

(i) Direct protection (ii) Indirect protection

Direct protection works are done directly on the banks such as-

Slope protection of embankment and upper bank, and

Toe protection of lower bank.

As such works continuously cover a certain length of banks; they are also called 'Continuous Protection'. Commonly seen direct protection works are banks protected against erosion by revetments or by a series of hard-points. Such bank protection is normally required to maintain

the existing bank line for economic or other human interests.

Indirect protection works are not constructed directly on the banks but in front of them in order to reduce the erosive force of the current either by

- Repelling Groynes- deflects the current from banks, or
- Sedimentation or Permeable Groynes- allows water to pass but not sediment. (These groynes have openings- so area is increased and the velocity of water is reduced. Therefore the water can no longer carry the sediment load and so the sediment is deposited.)

Examples of typical bank protection structures are:

- groynes,
- longitudinal dikes
- bank protection by means of revetments,
- cross dikes tying in longitudinal structures to the bank to divide the closed-off channel spaces,
- sills to stabilize the bottom of the regularized river according to a corresponding longitudinal slope,
- closures to cut off secondary channels,
- bed load traps: structures to trap and stabilize bed-load and causing its elevation (Przedwojski et al., 1995).

Indirect protection works are not used now-a-days in Bangladesh as they failed to protect the river bank. Therefore, direct protection works are usually followed to fulfill this purpose.

2.3 Revetment and Riprap Structures

Revetment is artificially roughening of the bank slope with erosion-resistant materials. A revetment mainly consists of a cover layer, and a filter layer. Toe Protection is provided as an integral part at the foot of the bank to prevent undercutting caused by scour. The protection can be divided as falling apron or launching apron, which can be constructed with different materials, e.g., CC blocks, rip-rap, and geobags. Figure 2.1 shows revetments and their different components.

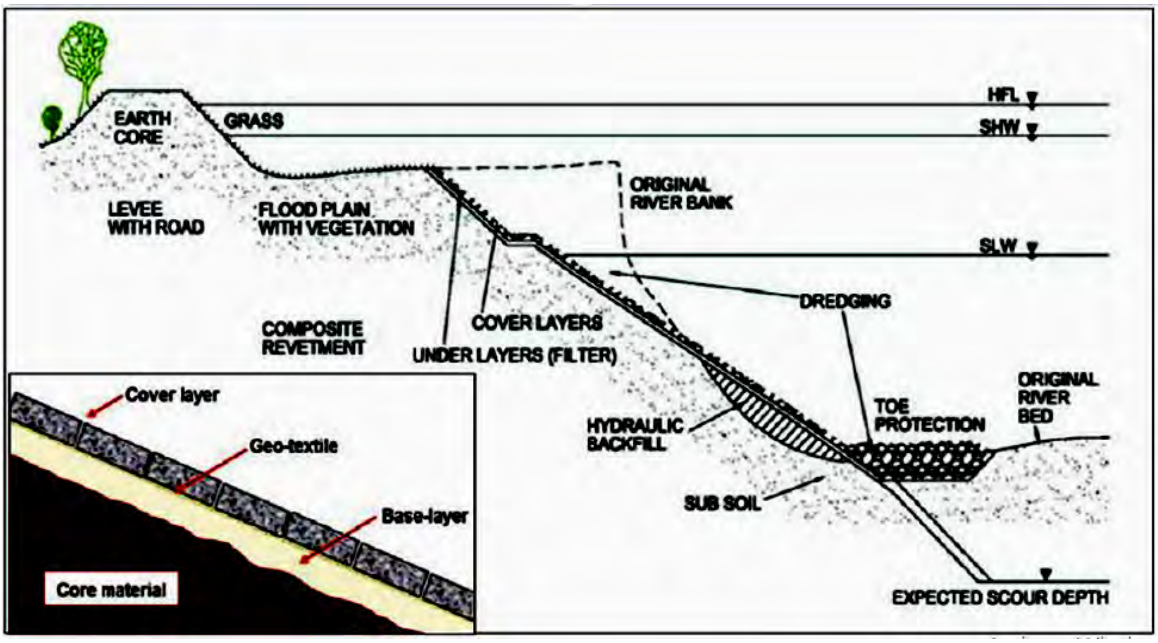

Figure 2.1: Components of a revetment works (Source: BWDB, 2010).

Launching apron consists of interconnected elements that are placed horizontally on the floodplain and normally anchored at the toe of the embankment. The interconnected elements are not allowed to rearrange their positions freely during scouring but launch down the slope as a flexible unit. The falling apron, on the other hand, consists of loose elements (e.g., CC blocks, geobags, stones) placed at outer end of the structure. When scour hole approaches the apron, the elements can adjust their position freely and fall down the scouring slope to protect it.

Riprap is the term given to loose armour made up of randomly placed quarried rock. It is one of the most common types of cover layer used all over the world. Riprap structures are attractive because their outer slopes force storm waves to break and thereby dissipate their energy. They are also used extensively because:

- Rock can often be supplied from local quarries.
- Relative ease of placing (including under water sites).
- Flexibility and to some extent self-repairing.
- Durability
- High roughness to attenuate waves and currents.
- Even with limited equipment, resources and professional skills, structures can be built that perform successfully.

- There is only a gradual increase of damage once the design conditions are exceeded. Design or construction errors can mostly be corrected before complete destruction occurs.
- Low maintenance and repair works are relatively easy and generally do not require mobilization of very specialized equipment.
- The structures are not very sensitive to differential settlements, due to their flexibility.
- Natural and environmentally acceptable appearance.

Riprap is made up of durable, angular stones ranging typically from 10 to 50 cm depending on the hydraulic loads. Its stability depends on the size and mass of the stones, their shape and gradation. The angular and cubical riprap stones show the best performance. Riprap mixture should form a smooth grading curve without a large spread between median and maximum sizes. It is normally placed in one, two or three layers, and a sub layer is often incorporated.

2.3.1 Choice of revetment

The type of material to be used for revetment depends upon the cost of materials, durability, safety and appearance. In many circumstances, attention is concentrated in Bangladesh on revetment because of its following advantages:

- It is flexible and is not impaired by slight movement of the embankment resulting from settlement.
- Local damage can be repaired easily.
- No special equipment or construction practices are necessary. Appearance is natural.
- Vegetation will often grow through the rocks.
- Additional thickness can be provided at the toe to offset possible scour.

2.3.2 Previous studies on geosynthetic products for revetment works

Raju (2011) Sixteen experimental runs with eight types of elements have been conducted for investigating incipient condition for discharges range from0.033 m^3/s to 0.052 m^3/s. An empirical relationship to determine the size of toe protection element based on incipient conditions developed. Equation 5.10 is used to generate values of the size of toe `protection elements. Ahmed. T (2014) incipient condition experiment in case of underwater construction. Square shaped bags required higher velocity to reach incipient condition than that of rectangular bags. Liu (1981) performed experimental analysis to determine impact force of waves on a 24 cases of complete impact forces striking on the test model occurred

which implied that breaking waves were reproduced before they just hit the model. An equation to describe the equilibrium shape of sand sausage is also presented. Kobayashi and Jacobs (1985) conducted model tests in a wave flume to examine the effects of berm type slopes on the stability of armour units and wave run-up, compared to those of uniform slopes. A simple analysis procedure based on the proposed method is developed, using the 'Equivalent Uniform Slope', for a preliminary design of a berm configuration. Klusman (1998) conducted an analysis of the circumferential tension of geosynthetic tubes. In general, the previous studies are quite limited, since they are largely related to typical aspects in terms of design and construction. In spite of growing applications of geobags or geocontainers, relevant studies are still lacking (Zhu et al., 2004).

2.3.3 Toe scour estimation and protection

Riprap protection for open channels is subjected to hydrodynamic drag and lift forces that tend to erode the revetment and reduce its stability. Undermining by scour beyond the limits of protection is also a common cause of failure. The drag and lift forces are created by flow velocities adjacent to the stone. Forces resisting motion are the submerged weight of the stone and any downward and lateral force components caused by contact with other stones in the revetment.

Lack of protection of the toe of the revetment against undermining is a frequent cause of failure of revetment. Therefore, protection of the toe of revetment by suitable method is a must. This is true not only for riprap, but also for a wide variety of protection techniques. The scour is the result of several factors including the factors mentioned below:

1. Change in cross-section in meandering channel after a bank is protected*:* after a bank is protected, the thalweg can move towards the outer bank and/or a channel with highly erodible bed and bank can experience significant scour along the toe of the new revetment.
2. Scour at high flows in meandering channel*:* Bed observed at low flows is not the same as that exists in high flows.
3. Braided Channels*:* Scour in a braided channel can reach a maximum at intermediate discharges where the flow in the channel braids concentrates along the protective work or attacks the banks at a sharp angle (USACE, 1994).

2.3.4 Toe protection methods of revetment

Toe protection of revetments may be provided by following methods:

(i)Extension to maximum scour depth: Lower extremity of revetment placed below expected scour depth or founded on non-erodible bed materials. These are preferred method, but can be difficult and expensive when underwater excavation is required.

(ii)Placing launchable stone: Launchable stone is defined as stone that is placed along expected erosion areas at an elevation above the zone of attack. As the attack and the resulting erosion occur below the stone, the stone is undermined and rolls/slides down the slopes, forming a surface cover layer reducing the erosion.

In general, the design implies that the scouring and undermining process of the developing scour hole in front of the structure initiates the deformation process of the toe protection. At the estimated maximum scour depth, the launching apron is assumed to cover and stabilize the bank-sided river profile, reducing further erosion of the bank.

2.3.5 Dimension of falling apron

Launching apron or falling apron has been considered to be the most economic and common method of toe protection of revetment. Falling aprons is a multilayer of protection element placed on a sloping or horizontal surface as protection against scour. Historically, surface as protection against scour. Starting from the limited understanding of spring the launched quantity was computed assuming a launched apron thickness similar to the thickness of pitching work above water. The quantities were calculated as geometrical area depending on launched thickness, depth of scour, and slope of the launching apron.

The slope of the launched apron was suggested by spring and Gales as 1:2 and according to Joglekar (1971) it should not be steeper, but also not flatter than 1:3. Different shapes and dimensions were suggested by the above mentioned authors for the apron to be placed in the river bed expecting/estimating a thickness of the launched apron as about 1.25 times the thickness of the slope cover layer. The face Slope of the launching apron may be taken as 2:1 for loose stone as suggested by spring. A schematic diagram an apron is shown in Figure 2.2 Table 2.1 presents a summary of these dimensions.

R' = HFL-LWL

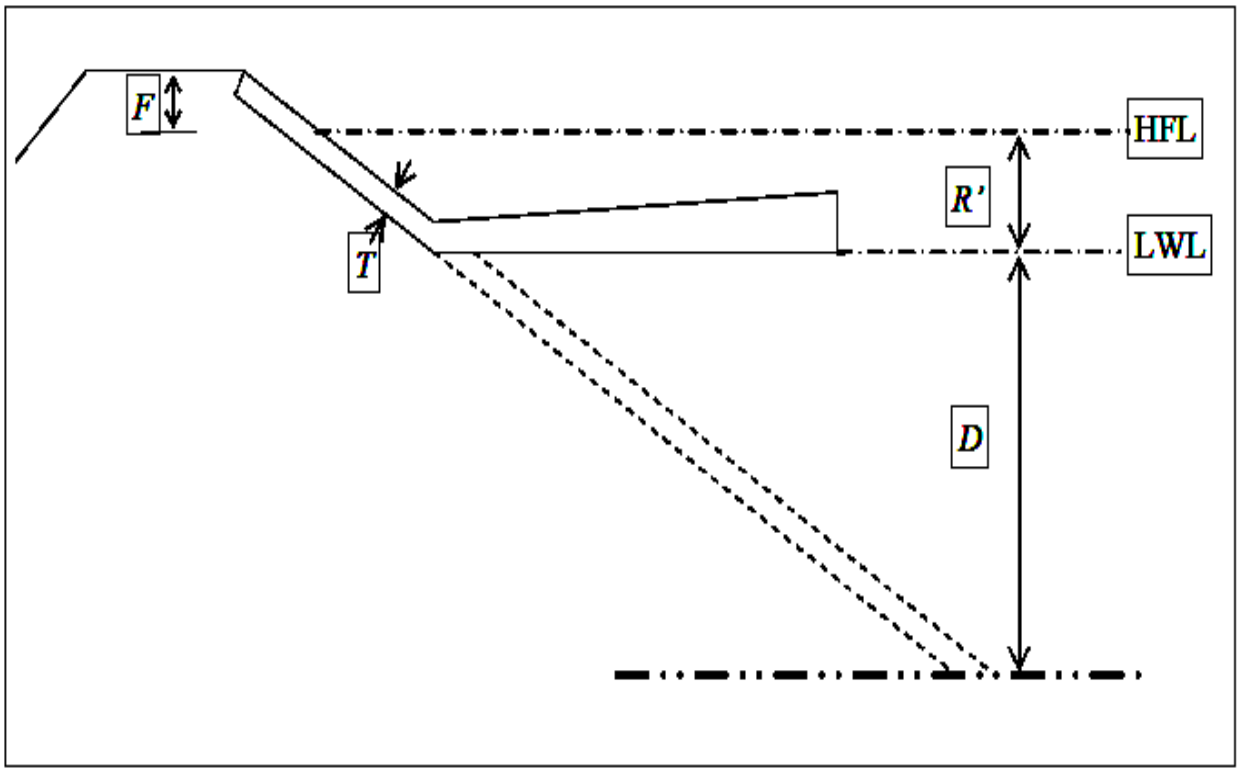

Figure 2.2: Schematic diagram of an apron.

2.3.6 Underwater toe protection construction

During construction of toe, geobags and CC blocks are delivered directly from vessel for placement of protective elements at designated position in the settling fashion. This process is simple but their dumping behavior plays a significant role. However, in such a condition identification of placement of protective elements in underwater flowing situation is found to be more difficult (Raju,2011). Toe protection work in river project side dumping geobags and CC blocks were observed and are shown in Photograph 2.1 and 2.2.

Photograph 2.1: Geobags are being dumped for toe protection.

Photograph 2.2: CC blocks on the construction site has been created for dumping.

2.4 Placement of Protection Elements

Placement of protection elements is mainly governed by its incipient condition under various hydraulic conditions. Hydrodynamic characteristics, especially the settling behavior of geobags and blocks, are of practical significance particularly for the construction of toe of a revetment and submerged groins or dikes. Study related to these hydrodynamic characteristics is very scarce in literature.

2.5 Incipient Condition

When the hydrodynamic force acting on a particle has reached a value that, if increased even slightly will put the particle into motion, critical or threshold condition are said to have been reached. When critical conditions obtain values of such quantities as the mean velocity, bed shear stress or the stage of a stream are said to have their critical or threshold values.

The driving forces are strongly related to the local near bed velocities. In turbulent flow conditions the velocities are fluctuating in space and time which make together with the randomness of both the particle size, shape and position that initiation of motion is not merely a deterministic phenomenon but a stochastic process as well.

- **Definition of incipient condition**

The definition of incipient condition is uncertain and ambiguous although the iniciation of motion due to tractive forces have been investigated to a great extent. The critical shear stress for initiation of motion occurs at the lowest shear stress that produces sediment transport is also a common misconception. Paintal (1971) and Lavelle and Mofjeld (1987) however, suggested from stochastic point of view that, due to fluctuation nature of instantaneous velocity, there is no mean shear stress below which there will be zero transport, with this consideration ,The critical minimal amount of transport.. Visual and reference techniques are the most common method of determining initiation of motion (Buffington 1999).

2.6 Incipient condition based on critical shear stress

The forces acting on a particle over which a fluid is flowing are the gravity forces of weight and buoyancy, hydrodynamic lift normal to the bed, and hydrodynamic drag parallel to the bed. The lift is often neglected without proper justification because both analytical and experimental studies have established its presence. Most treatments of forces on a particle on a bed consider only drag; lift does not appear explicitly. But, because the

constants in the resulting theoretical equations are determined experimentally and because lift depends on the same variable as drag, the effect of lift regardless of its importance is automatically considered (Raju 2011).

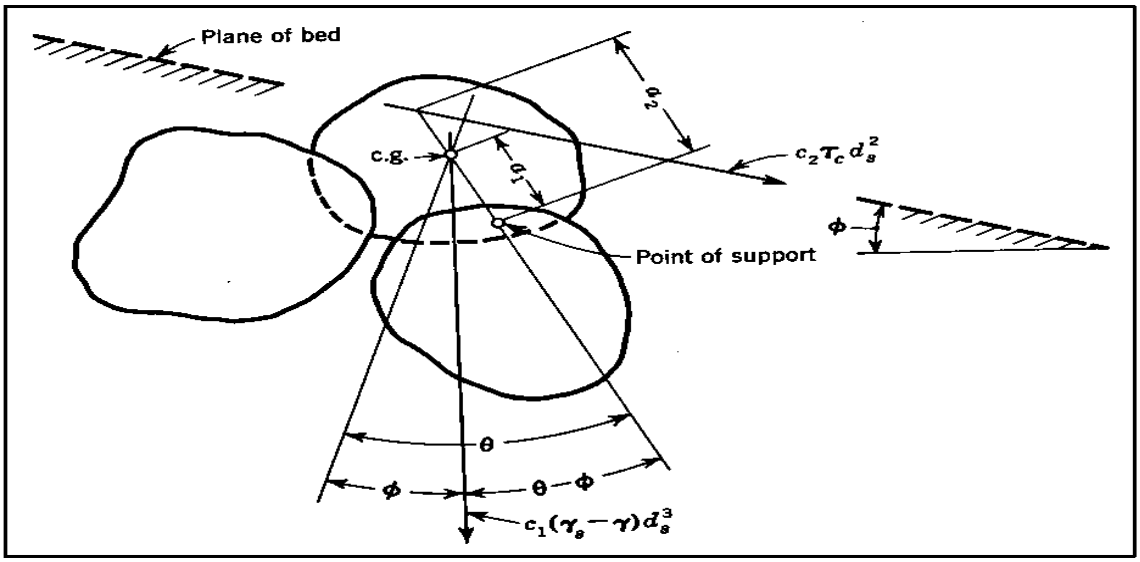

Figure 2.3: Forces on particle in flowing stream (Source: Vanoni, 1975)

The forces on a particle on the bed is depicted in Figure 2.3, in which ϕ = the slope angle of the bed; and θ = the angle of repose of the particle submerged in the fluid,

And intergranular forces are ignored. The particle will be moved or entrained if the hydrodynamic forces overcome the resistance. When motion is impending, the bed shear stress attains the critical or competent value, τc, which is also termed the Critical tractive force. Under critical conditions, also, the particle is about to move by rolling about its point of support. The gravity or weight force is given by

$$W = C_1(\gamma_s - \gamma)d_s^3 \tag{2.1}$$

in which $c1 d_s^3$ = the volume of the particle where $c1$ is a constant; d_S = its size, usually taken as its mean sieve size; and γ and γ_S = specific weights of fluid and sediment, respectively. The critical drag force is

$$F_D = c_2\tau_c d_s^2 \tag{2.2}$$

in which $c2{d_S}^2$ = the effective surface area of the particle exposed to the critical shear stress, τ_C where $c2$ is a constant. Equating moments of the gravity and drag forces about the support yields:

$$W a_1 \sin(\theta - \emptyset) = F_D a_2 cos\theta$$

$$C_1(\gamma_s - \gamma) d_s^3 a_1 \sin(\theta - \emptyset) = c_2 \tau_c d_s^2 a_2 cos\theta$$

$$or,\ \tau_c = \frac{c_1}{c_2}\frac{a_1}{a_2}(\gamma_s - \gamma) d_s \cos\emptyset(tan\theta - tan\emptyset) \quad (2.3)$$

For a horizontal bed, $\phi = 0$, and Equation (2.3) becomes:

$$\tau_c = \frac{c_1}{c_2}\frac{a_1}{a_2}(\gamma_s - \gamma) d_s tan\theta \quad (2.4)$$

When *a1* and *a2* are equal the forces on the particle act through its center of gravity and the fluid forces are caused predominantly by pressure. Also, when *a1* and *a2* are equal it will be seen that the ratio of the forces on the particle parallel to the bed i.e. hydrodynamic force, to those acting normal to the bed i.e. immersed weight, is equal to *tan θ*, resulting Equation (2.4) as:

$$c\ tan\theta = \frac{\tau_c}{(\gamma_s - \gamma) d_s} \quad (2.5)$$

The left-hand side of equation (2.5) represents the ratio of two opposing forces: hydrodynamic force and immersed weight, which governs the initiation of motion.

Major variables that affect the incipient motion include τ_c, d_s, γ_s-γ, ρ and v. From dimensional analysis they may be grouped into the following dimensionless parameters

$$F\left[\frac{\tau_c}{(\gamma_s - \gamma)d}, \frac{(\tau_c)^{1/2}}{v}\right] = 0 \quad (2.6)$$

$$or,\ \frac{\tau_c}{(\gamma_s - \gamma)d} = F\left(\frac{U_{*c}\ d}{v}\right) \quad (2.7)$$

Where $U_{*c} = \sqrt{(\tau_c/\rho)}$ is the critical friction velocity. The left-hand side of this equation is the dimensionless critical Shields stress, τ_{c*}. The right-hand side is called the critical boundary Reynolds number and is denoted by R*c. Figure 2.4 shows the functional relationship of equation(2.7) established based on experimental data, obtained by Shields (1936) and other investigators, on flumes with a flat bed.

It is generally referred to as the Shields diagram. Each data point corresponds to the condition of incipient motion.

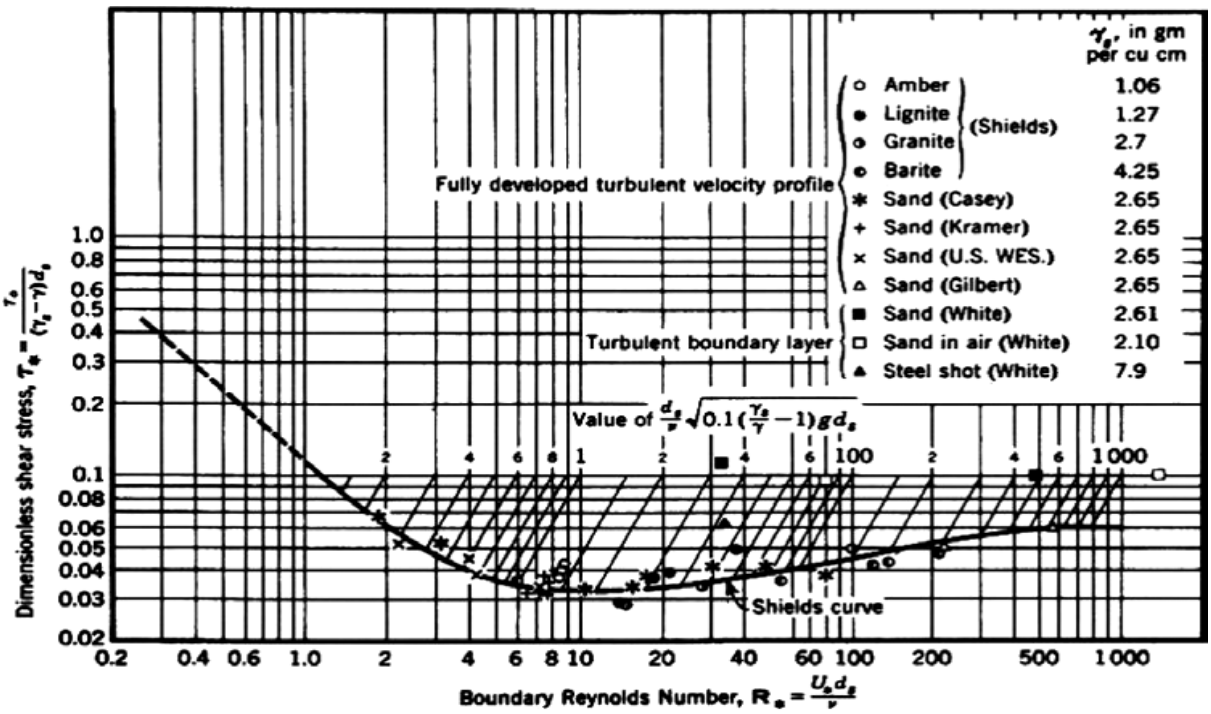

Figure 2.4: Shield's diagram for incipient motion (Source: Chang, 1992).

2.7 Incipient condition based on critical depth averaged velocity

The earliest studies were related to critical velocities of stones (Brahms, 1753 and Sternberg, 1875). They studied the critical near bed velocity and found that it was related to the particle diameter, as follows:

$$u_{oc}{}^2 \sim d_S$$

in which u_{oc} is the fluid velocity near the bed under critical conditions. Taking

$$\tau_c \sim u_{oc}^2$$

and substituting this in Equation (2.5) also gives:

$$u_{oc}^2 \sim d_s$$

Cubing both sides of the relation gives:

$$(d_s^3 \sim U_{oc}^6)$$

Which is the well known sixth power law. Because the volume or weight of a particle is proportional to d_s^3, the law states that the weight of largest particle that a flow will move is proportional to the sixth power of the velocity in the neighborhood of the particle. Rubey (1948) found that this law applied only when d_s is large compared with the thickness of the laminar sub layer and the flow about the grain is turbulent.

The near bed velocity is, however, not very well defined and it is preferable to use the critical depth averaged velocity $(\overline{u_c})$ as the characteristic parameter. It can be derived from the critical bed shear stress using the Chezy equation. Assuming hydraulic rough flow

conditions $\left(\frac{u_* k_s}{v} > 70\right)$ the critical depth averaged flow velocity for a plane bed can be expressed as:

$$\overline{u_c} = 5.75\, u_{*,c} \log\left(\frac{12h}{k_s}\right) \quad (2.8)$$

Where $\overline{u_c}$ = critical depth averaged flow velocity; h = water depth; $k_s = \alpha d_{90}$ = effective bed roughness of a flat bed; α = coefficient (α = 1 for stones $d_{50} \geq 0.1$ m and α = 3 for sand and gravel material); $u_{*c} = (\tau_{*c})^{0.5} (\Delta g d_{50})^{0.5}$ = critical bed shear velocity; and τ_{*c} = critical Shields parameter. Equation (2.8) can be expressed as:

$$\overline{u_c} = 5.75\, (\Delta g d_{50})^{0.5} (\tau_{*c})^{0.5} \log\left(\frac{12h}{k_s}\right) \quad (2.9)$$

Using Equation (2.9), $k_s = 3d_{90}$ and $d_{90} = 2d_{50}$ and the Shields curve, the critical depth averaged velocity can be expressed as:

$$\overline{u_c} = 0.19\, (d_{50})^{0.1} \log\left(\frac{12h}{3d_{90}}\right) \quad \text{for } 0.0001 \leq d_{50} \leq 0.0005m \quad (2.10)$$

$$\overline{u_c} = 8.50 (d_{50})^{0.6} \log\left(\frac{12h}{3d_{90}}\right) \quad \text{for } 0.0005 \leq d_{50} \leq 0.002m \quad (2.11)$$

Where d_{50} = median particle diameter; d_{90} = 90 % particle diameter.

2.7.1 Analysis of Incipient Motion

Neil and Hey (1982) have noted that many engineers prefer design procedures based on velocity. The appropriate velocity for use in the riprap design procedure must be determined. The velocity used must be representative of flow conditions at the riprap and must be able to be determined by the designer by relatively simple methods. Local bottom velocity is the most representative velocity but is difficult for the designer to predict. Local average velocity, also called depth-averaged velocity is representative of flow conditions at the point of interest and can be estimated by the designer (Maynord et al., 1989).

The dimensional analysis follows the analyses previously presented by Neill (1967). The pertinent variables applicable to the stability of coarse particles are

$$f(h, d, \rho_w V, \gamma' s, v) = 0 \quad (2.12)$$

where h = depth of flow; d = characteristic particle size; ρ_w = water density; V = characteristic velocity; γ'_s = submerged specific weight of particle; and v = kinematic viscosity. By requiring rough turbulent flow, the viscosity effects are eliminated and the dimensionless ratios are found to relate in the following form:

$$\frac{d}{h} = f\left[\left(\frac{\gamma_w}{\gamma_{s-\gamma_w}}\right) \quad \frac{V}{\sqrt{gh}}\right] \quad (2.13)$$

Where γ_s = specific weight of particle = $g\rho_s$. In this study, the pertinent variables are as shown in equation (2.12) with the repeating variables of *V, d*, and γ'_s.

Equation (2.13) is presented in the same form in Bogardi (1978). The right side of equation (2.13) contains a local Froude number. Almost all riprap problems concern subcritical flow and that reduces the significance of defining this as a Froude number.

2.7.2 Incipient condition of sediment particles

- **Shear strees:**

A simple theoretical description for the initiation of movement of non cohesive particles of uniform size is given by chepil (1959), and that approach is followed here. In this analysis it is assumed that a spherical particle of diameter d rests on other spherical partials of diameter *d*. A gravitational force F_g acts through the center of the sphere at point O. The drag force F_d and lift force F_l do not generally act through the point O and are assumed to act through the point O, some distance above O, At initiation of movement of the particle, the moment about point p of the forces acting on the particle must be zero, or

$$F_d b = (F_g - F_l)a \tag{2.14}$$

Where a=horizontal distance between *O, O',* and *P*, and *b*=vertical distance between *O'* and *P*
The gravitational force has a magnitude of

$$F_g = (F_g - F_l)a \tag{2.15}$$

Where g=gravitational constant and $C_3 = \pi(\rho_s - \rho_w)g/6$ and is equal to $8.21X10^3\ N/M^3$ when it is assumed that $\rho_s = 2.6kg/l$ (particle density) and ρ_w =1.0 kg/l (water density) chepil (1959) has stated that Flis approximately $.085F_d$. Saffiman (1965) theoretical determined the lift force on a sphere in an unbounded shear flow using asymptotic expansions .For low shear stresses of the magnitude considered here, the lift force that he calculated is much smaller than that predicted by Chepil. Whether F_l is negligible or give by $0.85F_d$ Eq (2.14) reduces to

$$F_d = c_2 F_g \tag{2.16}$$

Where C=constant of order one.
The drag force is usually written as

$$F_d = \frac{1}{2}\rho_u C_d 4u^2 \tag{2.17}$$

Where C_d =drag coefficient; A=cross-sectional area of the sphere and is give by $\pi\frac{d^2}{4}$ and $u =$

fluid speed. The drag force per unit area of the bed, or share stress, is generally expressed as $= CU^2$, where C= another drag coefficient. From these definitions the above equation can be written by.

$$F_d = C_1 \tau d^2 \quad (2.18)$$

Where $C_1 = \frac{\pi p_a C_d}{8C}$

By substituting Eq (2.18) into Eq. (2.16) and rearranging, one obtains

$$\tau_{en} = \frac{c_2}{C_1} \quad \frac{F_g}{d^2} \quad (2.19)$$

Where τ_{en}=critical shear stress for the initiation of movement of no cohesive particles, Eq. (2.15) substitute into the above equation

$$\tau_{en} = \frac{c_2 c_3}{C_1} \quad d = constant\ d \quad (2.20)$$

As indicated above this constant has been determined from experiment and more Refined theoretical analyses which have taken into account turbulent fluctuation and the relative protrusion of protrusion of particles (Grass 1970; Fenton and Abbott 1977 chin and Chiew 1993); it has the approximate value of 0.414X10^3 N/m^3

.

- **Tests with Regular waves**

Observed values of the incipient depth of motion h_d were evaluated to determine the effects of various variables, with the following results.

1. The water depth h has no appreciable effect on h_d in the range covered in the tests. This result confirms the findings of van Hijum and Pilarczyk (1982).
2. The h_d increases with the increase of the wave height H.
3. The h_d decreases with the increase of the particle size D.
4. The increase of the wave period T causes to h_d increase. This may be explained by breaking of longer waves at large depths.
5. The h_d values recorded for the slope tan α =0.15 are smaller than those for tan α = 0.20, other conditions remaining the same.

To determine the functional relationship in $S_b = \frac{h_d}{D.sin\alpha} = f(_{N\ ii}\varepsilon)$, all the experimental result (Unal 1996)are plotted on the ln(ln)N_s ln ϵ plane. It is seen that points for both tan α =0.15 and tan α =0.20 with equal values of the threshold damage level S_b lie on straight lines of slope-0.5

$$\ln(N_c) = -0.5 \ln \in + c \quad (2.21)$$

Where C=a function of S_b given by the regression equation.

(Correlation coefficient = 0.998)

$$C = \ln(0.197.S_b + 1.173 \quad (2.22)$$

Combining (2.21), and (2.22), the following equation is obtained for the incipient depth of motion under regular waves.

$$\frac{h_d}{D} = \frac{\sin \propto}{0.179} \left(N_s\sqrt{\in} - 1.173\right) \quad (2.23)$$

The Combination of the parameters $N_s\sqrt{\in}$ also appears in the formula given by van der Meer (1993) for the probabilistic design of breakwater armour layers.

- **Tests with irregular waves**

In the case of irregular waves, a similar analysis leads to the following expression (correlation coefficient =0.996):

$$\frac{h_d}{D} = \frac{\sin \propto}{0.148} \left(N_s\sqrt{\in} - 0.915\right) \quad (2.24)$$

Placed rock as protection against erosion by flow down steep slopes (Riprap)

- **Methodology (Armor characterization)**

Two size of sandstone and a single size of crushed basalt wear obtained from local quarries and sorted to ensure a coefficient of uniformity less than 2.3. After trans port from quarry to set. Location, the sandstone appeared to be significantly less angular than the basalt. Each rock sample was carefully tested to obtain the characteristics summarized.

Random dumping was achieved by dropping then scraping rock along the slope with the objective of achieving a similar physical arrangement to large scale material dumped using construction equipment. Placement was achieved manually by carefully arranging the rocks to minimize the porosity of the armor blanket. The average thickness of the two rock layer from the top of any underlying filter to the top of the armor was $1.60d_{50}$ to $1.86d_{50}$ for the random and placed configuration.

- **Randomly dumped armor failure:**

Rock armor failure, defined as exposure of the filter below the armor, is the conventional basis for protection design.(e.g, Abt and johnson1991). The stability equation coefficient of Peirson and Cameron (2006) for failure of random dumped rock must be,

$$v_c = 0.88\sqrt{2g(\rho_s} - \rho)/\ \sigma p\sqrt{d_{50}}\cos\theta\sqrt{tan\varphi - tan\theta} \quad (2.25)$$

Where φ = angle of friction of the rock; ρ= density of water; and ρ_s =density of the rock.

- **Incipient motion of sediment particles over fixed beds**

The particle critical Froude number $V_c/\sqrt{gd(S_s - 1)}$

$V_c/\sqrt{gd(S_s - 1)}$ =0.61$(d/R)^{-0.27}$

For both the channel shapes with smooth beds over a range of 0.01< $d/R < 1$

2.7.3 Incipient condition of erosion protection elements

Inglis (1921) proposed a relationship for incipient motion of a single layer of stones on a flat bed on the basis of small scale experiments as:

$$\frac{d_{50}}{h} = 0.34\left[\left(\frac{\gamma}{\gamma_{s-\gamma}}\right)^{0.5}\frac{V}{\sqrt{gh}}\right]^{2.6} \quad (2.26)$$

Where d_{50} = medium size of stone; V = depth averaged flow velocity; g = gravitational acceleration; and h = depth of flow.

On the basis of experiments with natural gravels, glass spheres and low density Spheres, Neil (1967) proposed a relationship designed to just maintain stability on a flat bed, which can be arranged in the form:

$$\frac{d_{50}}{h} = 0.32\left[\left(\frac{\gamma}{\gamma_s-\gamma}\right)^{0.5}\frac{V}{\sqrt{gh}}\right]^{2.5} \quad (2.27)$$

Maynored (1989) presented a relationship on the basis of more extensive experiments at larger scales, for incipient movement of riprap

$$\frac{d_{50}}{h} = 0.30\left[\left(\frac{\gamma}{\gamma_{s-\gamma}}\right)^{0.5}\frac{V}{\sqrt{gh}}\right]^{2.5} \quad (2.28)$$

Where d_{30} = riprap size for which 30% is finer by weight.

USACE (1991) modified the Maynord equation, replacing the primary coefficient. 0.30 by a set of four multiplying coefficients and inserting a side slope correction factor, to obtain a relationship that can be arranged as follow.

$$\frac{d_{30}}{h} = S_f C_s C_v C_T \left[\left(\frac{\gamma}{\gamma_{s-\gamma}}\right)^{0.5} \frac{V}{\sqrt{k_1 g h}}\right]^{2.5} \quad (2.29)$$

Maynored (1989) presented a relationship on the basis of more extensive experiments at larger scales, for incipient movement of riprap

$$\frac{d_{50}}{h} = 0.30 \left[\left(\frac{\gamma}{\gamma_{s-\gamma}}\right)^{0.5} \frac{V}{\sqrt{g h}}\right]^{2.5} \quad (2.30)$$

Where d_{30} = riprap size for which 30% is finer by weight.

USACE (1991) modified the Maynord equation, replacing the primary coefficient. 0.30 by a set of four multiplying coefficients and inserting a side slope correction factor, to obtain a relationship that can be arranged as follow

$$\frac{d_{30}}{h} = S_f C_s C_v C_T \left[\left(\frac{\gamma}{\gamma_{s-\gamma}}\right)^{0.5} \frac{V}{\sqrt{k_1 g h}}\right]^{2.5} \quad (2.31)$$

Where V = depth averaged velocity; S_f = safety factor, minimum recommended value for riprap design = 1.1; C_s = stability coefficient for incipient failure having a value of 0.30 for angular rock and 0.36 for rounded; C_V = coefficient for vertical velocity distribution, range 1.0 to 1.28 for straight channels to abrupt bends; C_T = coefficient for riprap layer thickness; K_1= side slope correction factor.

Remarks :

Erosion is one of many natural river processes. Problem arises where the rate of erosion is considered too rapid to be acceptable. This can be problematic for a number of reasons, for instance loss of valuable agriculture land, risk to local infrastructure and sedimentation downstream.

Construction work among river bank protection works is the main task. In need to have knowledge to clean the river of the incipient condition, Toe protection components are thrown into the water flowing from the ship. Then there is where the river lies beneath the river.

It is necessary to know how to remove the protection items underwater. In order to establish the material the right knowledge can be achieved. Geobags and blocks have a lot of real importance. A cover is provided to protect the toe. That's why more attention about groins or dikes. Tried to conduct experimental investigation to understand the above objectives of this research.

The theoretical basis of governing parameters of incipient condition has been analyzed in this chapter. Detail of the experimentation, measurements and observations is reported in chapter three. Measured data from experiments will be used to obtain empirical relationships using equations.

CHAPTER THREE

METHODOLOGY

3.1 Introduction

This chapter describes the detailed experimental setup, experimental procedure and data collection techniques. A brief description of the experimental design, procedure and observation is depicted here.

3.2 Outline of the methodology

The study has been carried out according to following steps of activities:

(i) Theoretical analysis of governing parameters
(ii) Design of experiments
(iii) Experimental setup
(iv) Test scenarios and experimental run
(v) Measurements and observations
(vi) Analysis of data and development of equations
(vii) Predictive performance of proposed equation and comparison with others

The stepwise methodology is explained in a flow diagram as shown in Figure 3.1.

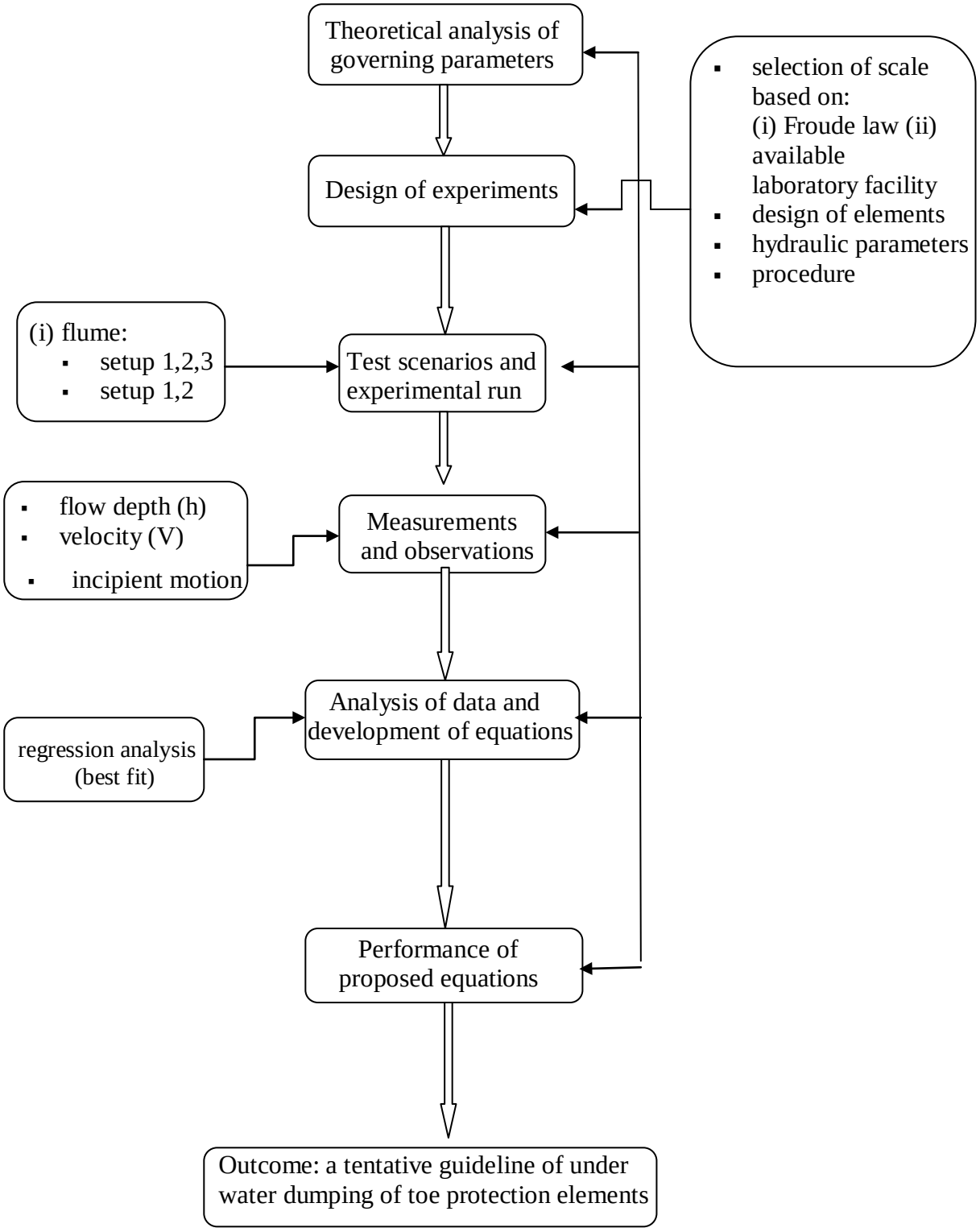

Figure 3.1: Flow diagram of methodology of the study.

3.3 Remarks

The theoretical basis of governing parameters of incipient condition has been analyzed in this chapter. Detail of the experimentation, measurements and observations is reported in chapter four. Measured data from experiments will be used to obtain empirical relationships using equations

3.4 Experimental Setup

The experiments are conducted in a incipient condition in the large tilting flume of the Hydraulics and River Engineering Laboratory of Water Resources Engineering Department, Bangladesh University of Engineering and Technology (BUET), Dhaka. Schematic diagram of the flume setup is shown in Figure 3.1.

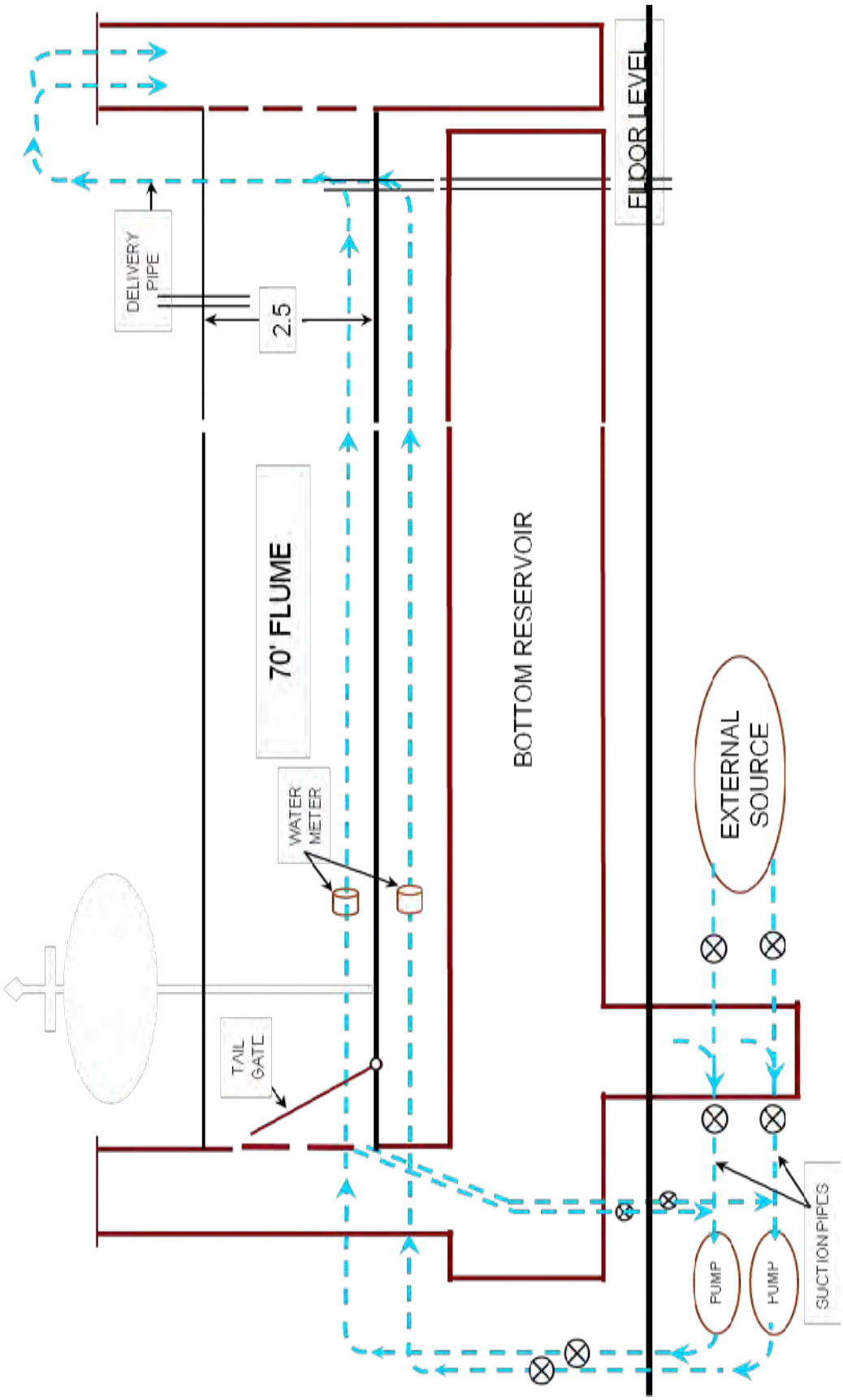

Figure 3.2: Schematic diagram of the experimental flume.

3.4.1 Flume setup

For the purpose of the data collection an experimental setup tilting flume, these precision engineered component are designed and fabricated using high grade material in the process. The experiment has been carried out in a effective length 70 ft, 2.5 ft wide and 2.5 ft deep rectangular tilting flume in the Hydraulics and River Engineering Laboratory.

The side walls of the flume are vertical and made of vertical clear glass. The bed is painted by water resistant color to avoid excess bed friction. A tail gate is provided at the end of the flume to control the depth of flow. Two pumps are there to supply water from the reservoir to the flume through a recirculation channel.

A photograph of the flume is shown in Photograph 3.2. Point gauge is used to measure the depth of flow. The gauge is mounted on a trolley laid across the width of the flume. The whole structure of point gauge could be moved over the side rails. The point gauge can measure with 0.10 mm accuracy.

Photograph 3.1: Laboratory flume.

3.4.2 Electromagnetic flow meter

Magnetic flow meter, also known as electromagnetic flow meter. Discharge measurements are taken from the electromagnetic flow meter in the unit m3/h. Magnetic flow meter is a volume flow rate meter for conductive fluids in pipelines. Also, It allows measurement of flow rates in both direction. Of the two flow meters one is 200 mm and 150 mm diameter. The flow through the pipe is controlled by the valve. Also advantage of using electromagnetic flow meter basically less maintenance. Photograph 3.3 shows an electromagnetic flow meter.

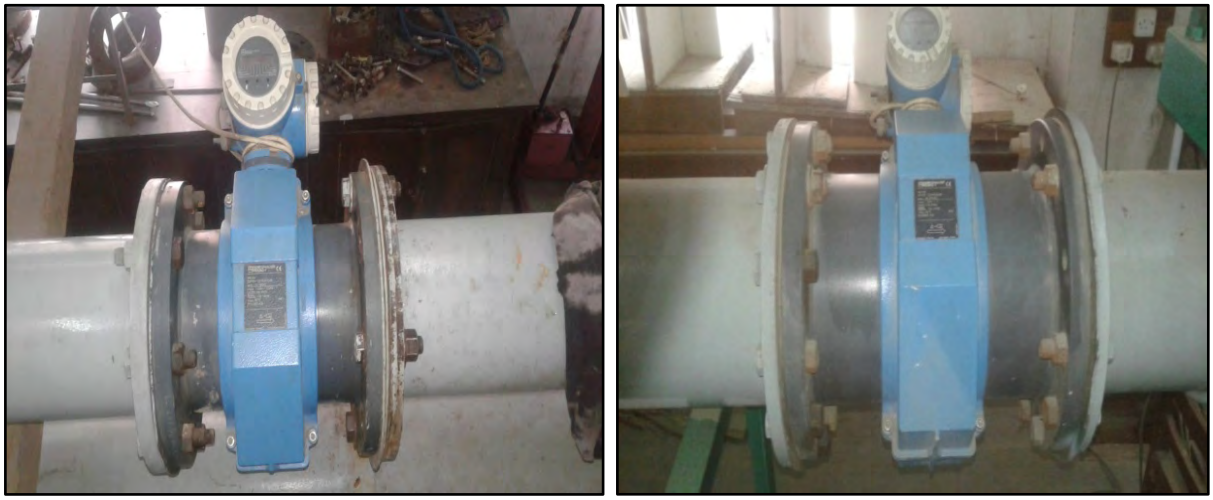

Photograph 3.2: Electromagnetic flow meter.

3.4.3 Current meter

Several classes of current meter are used in water measurement. A small current meter is used for velocity measurement. It consists of three basic parts: 50 mm diameter propeller, 1 m long 9 mm diameter rod and signal counter set. Minimum depth of water for using the instrument is approximately 4 cm. It is capable of measuring velocity from 3.5 cm/s to 5 m/s. Time and impulse measurement accuracy is ±0.01 seconds and ±0.5 impulses, respectively. Photograph 3.4 shows the current meter in the flume.

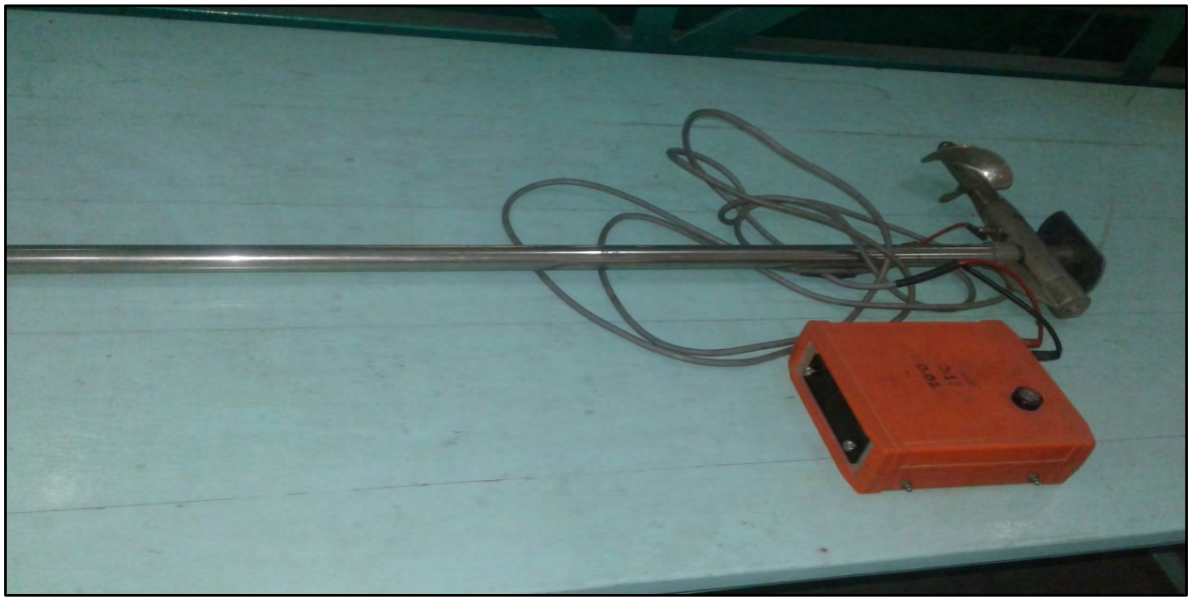

Photograph 3.3: Velocity measurement using current meter.

3.5 Experimental Size of Protection Elements

Following sections describe the process to determine the dimension of blocks and geobags.

3.5.1 Selection of scale for experimentation

A geometrically similar undistorted scale factor 20 has been selected to conduct the experiment. The present study determines the scale, model parameters, dimension etc. following Raju (2011). This selection of scale is based on (i) the available laboratory flume facilities and (ii) the Froude law criteria.

3.5.2 Design of various model parameters

From the above considerations, various scale ratios of model parameters are designed as shown in Table 3.1.

Table 3.1: Scale ratios of model parameters.

Quantity	Dimension	Scale ratio
Length	L	1:20
Volume or weight	L^3	1:8000
Velocity	$L^{1/2}$	1:4.47
Discharge	$L^{5/2}$	1:1789

It is assumed that the material and porosity remain unchanged for the experiment and Prototype. Therefore, protection elements used for the laboratory experiment should be the same as those designed for field construction except for the reduced dimension.

3.5.3 Design of size of sand cement block

Different blocks used for the present study is shown in Photograph 3.5. The dimensions of blocks are 23mm (C1), 20mm (C2) and 15mm (C3). Details are available in Raju (2011).

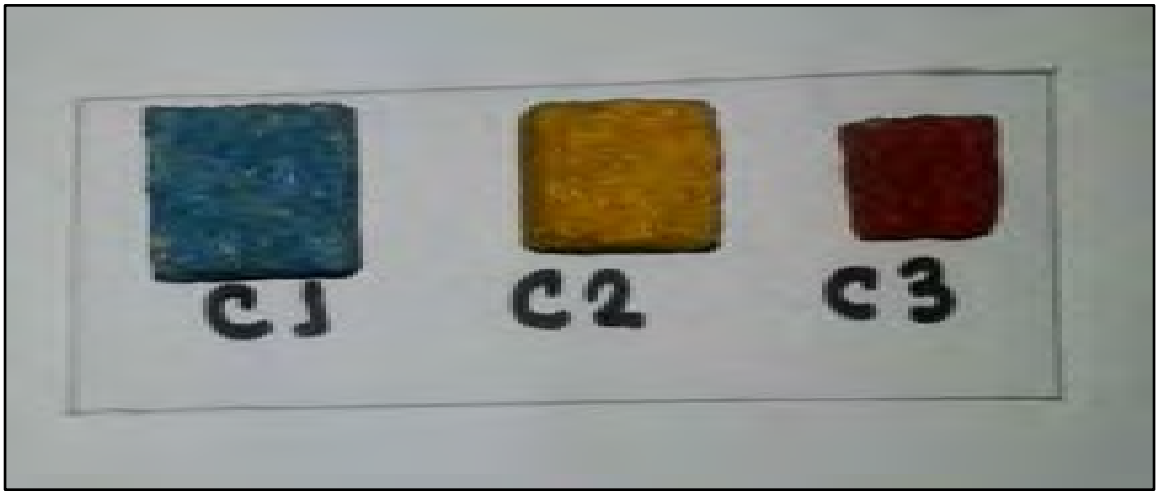

Photograph 3.4: Various sizes of CC blocks.

Different methods regarding calculations of unit dimensions of revetment cover layers and toe protections (e.g. PIANC, 1987; Pilarczyk, 1989; FAP 21/22, 1993) show only marginal deviations within the range of application for the rivers of Bangladesh. Since the widely used Pilarczyk formula (Pilarczyk, 1989; Przedwojski et al., 1995) includes the turbulence intensity, velocity and shear stress, it is followed to determine the nominal thickness of a protection unit. The formula is:

$$D_n = \frac{\emptyset_c K_T K_h}{\Delta K_s} \quad \frac{0.035\, u^{-2}}{\theta_c\, 2\, g} \qquad (3.1)$$

The values of the parameters of the formula are considered according to Zaman and Oberhagemann (2006). Here, D_n = nominal thickness of protection unit, m; φ_c = stability factor = 0.75 for continuous protection of loose units; K_T = turbulence factor = 1.5 for nonuniform flow with increased turbulence; K_h = depth and velocity distribution factor= $(h/D_n + 1)^{-0.2}$, h = water depth, m; Δ = relative density of protection unit $(\rho_s - \rho)/\rho = 1$; K_s = slope reduction factor $= \sqrt{(1 - sin^2\alpha / sin^2\emptyset)}$ = 0.72, α = slope angle = 26.57^0 (for 1V:2H); $\backslash$ = angle of repose = 40^0 (for blocks);

θ_c = critical value of dimensionless shear stress = 0.035 for free blocks; ū = depth averaged flow velocity, m/s. Details calculation is shown in Appendix A.

3.5.4 Design of size of geobag

The shape of geobag is rectangular and square. The length to width ratio ranges from 1.73 to 1.09. For some typical block sizes, the equivalent sizes of geobags are provided in FAP 21 (2001). Consequently block type C1 and C2 is equivalent to geobag type G1, G2 and G3, G4, respectively. The dimensions of the bags are 25mm (A1), 25mm (A2), 23mm (A3), 24mm (A4) and 20mm (A5). Photograph 3.5 shows different bags used in the experiment.

Photograph 3.5: Various sizes of geobags.

Photograph 3.6: CC blocks and geobags used in experiments.

3.5.5 Design of apron

Design scour depth can be estimated by Lacey's regime formula as it is widely used in this subcontinent in unconstructed alluvial rivers. This empirical regime formula is:

$$R = 0.47(Q/f)^{1/3} \quad (3.2)$$

With $D_s = XR\text{-}h$ (3.3)

Where D_s = Scour depth at design discharge, m; Q = Design discharge, m^3/s; h = Depth of flow, m; may be calculated as (HFL-LWL); f = Lacey's silt factor = $1.76\ (d_{50})^{1/2}$; d_{50} = Median diameter of sediment particle, mm; X = Multiplying factor for design scour depth.

Table 3.2: Hydraulic parameters of typical field condition.

High Water Level, HWL	9.0 m PWD
Low Water Level, LWL	3.0 m PWD
Design discharge, Q	20,000 m^3/s
Median diameter of sediment particle, d_{50}	0.12 mm
Multiplying factor for design scour depth, X	1.25 for straight reach of channel

Considering a typical field condition presented in Table 3.4 and from equation 3.2 and 3.3, D_s = 9.75 m. Therefore,

Width of apron, $W_{apron} = 1.5\ D_s$ = 14.63 m.

Width of apron in the flume, W_{apron} = 14.63/20 = 73 cm.

Thickness of protection over scoured slope, $T = 1.25\ D_n$.

Shape of the apron for blocks is followed according to Rao, 1946, discussed previously and shown in Figure 3.2.

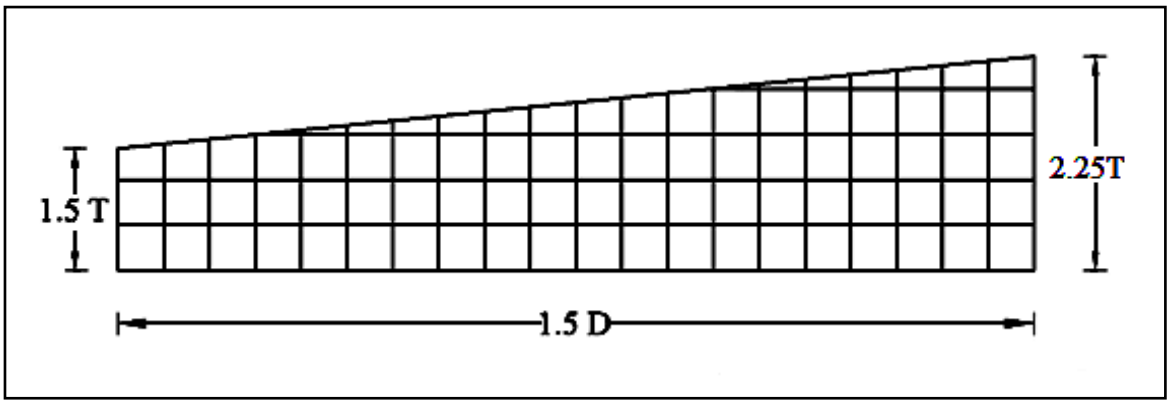

Figure 3.3: Schematic diagram for shape of apron for CC block**.**

Quantity of block:

Inside thickness of apron = 1.5 T

Outside thickness of apron = 2.25 T

Quantity of block, $V_{block} = L\ (1.5T + 2.25T)/2$ m^3/m Number of block per unit length = V_{block}/D_n^3

This amount of block is dumped so as to achieve the shape according to Figure 3.2,

over the width of apron per unit length to investigate its threshold condition.

Quantity of geobag:

In mass dumping concept, a falling apron is developed from the water line by dumping a calculated quantity of geobags as a heap below LWL along the river section. The geobags are assumed to launch in a slope of 1V:2H, to cover the slope and future scour holes. According to Halcrow and Associates (2002), a protection thickness of 0.61 m on the scour surface for a scour depth up to 17 m is required. For a typical condition as mentioned above, the calculated scour depth is 9.75 m.

Therefore,

Volume of geobag, $V_{geobag} = (10^2+20^2)^{0.5}$ x 0.61 m^3/m Number of geobag per unit length = V_{geobag}/D_n^3

This amount of geobag is dumped from the water surface over the width of apron per unit length in the flume to investigate its threshold condition.

3.5.6 Hydraulic parameters

Utility of an experimental investigation infield practice lies in the simulation of the field situations in the experimental setup. In order to simulate field conditions observed in different bank protection works already undertaken in Bangladesh, it is necessary to keep the velocity, water depth within a range. The flow depth is selected considering the High Water Level (HWL) and Low Water Level (LWL) in a typical field condition. This will facilitate the tasks of engineers and researchers to compare the test results with the field circumstances and to search for the option best suited for a given site condition for sustainable bank protection works. The hydraulic parameters are presented in Table 3.5.

For incipient motion experiments the hydraulic parameter is set based on the typical field Low Water Level (LWL) condition and is given in Table 3.6.

Table 3.3: Initial hydraulic parameters regarding experiment of incipient condition.

Type of element	Flume discharge, Q (m^3/h)	Experimental value		Corresponding field value	
		Depth of flow, h (m)	Velocity, V (m/s)	Depth of flow, h (m)	Velocity, V (m/s)
CC Block	150	0.23	0.35	4	1.56
CC Block	150	0.25	0.35	3	1.56
Geobag	150	0.25	0.29	4	1.33
Geobag	150	0.30	0.29	3	1.33

3.5.7 Test scenario

Duration of a run for incipient condition, tests and the duration of a run is about 125 minutes to 150 minutes for geobags and 120 minutes to 135 minutes for CC blocks, depending on their sizes.

Table 3.4: Test scenarios for incipient motion.

Run no.	Type of Protection Element	Initial Depth of Flow h(m)	Depth of flow (m)	Velocity (m/s)	Discharge (m^3/h)
1	**G1 (Geobag)**	**0.25**	**0.37**	**0.661**	**0.167**
2	**G2**	**0.25**	**0.35**	**0.579**	**0.147**
3	**G3**	**0.25**	**0.43**	**0.646**	**0.164**
4	**G4**	**0.25**	**0.41**	**0.629**	**0.159**
5	**G5**	**0.25**	**0.36**	**0.662**	**0.168**
6	**G1**	**0.3**	**0.43**	**0.588**	**0.149**
7	**G2**	**0.3**	**0.435**	**0.610**	**0.154**
8	**G3**	**0.3**	**0.45**	**0.629**	**0.159**
9	**G4**	**0.3**	**0.4**	**0.629**	**0.159**
10	**G5**	**0.3**	**0.425**	**0.557**	**0.141**
11	**C1 (CC block)**	**0.25**	**0.38**	**0.709**	**0.965**
12	**C2**	**0.23**	**0.375**	**0.752**	**0.066**
13	**C3**	**0.315**	**0.505**	**0.523**	**0.071**
14	**C1**	**0.18**	**0.295**	**0.762**	**0.193**
15	**C2**	**0.25**	**0.4**	**0.740**	**0.187**
16	**C3**	**0.33**	**0.47**	**0.569**	**0.144**
17	**C3Two Layer Place**	**0.25**	**0.4**	**0.661**	**0.167**
18	**C3Two Layer Place**	**0.28**	**0.4**	**0.672**	**0.170**

3.6 Procedure followed for incipient motion experiment

1. The components required for each unit length are determined. These amounts of components are dumped while running.
2. The common five types of geobags and three types of CC blocks are used. Geobags & CC blocks are investigated separately in the lab. The elements are removed from the surface up to four (4) cm above the water.
3. Green, red and yellow blocks are dumped in two times. But one experiment running.
4. Discharge flow meter two types are used. A discharge flow meter is set to define 150 meter cube per hour and the tail gate is fixed. The Fluid velocity is determined by the current meter at three location and the three heights.
5. The flow of the water gradually increases of 5 meter cube per hour and it was observed for 5 to 8 minutes. If the block is not movement then the water flow is increased.
6. When the water flows, the block or geobag are shake. Then the elements are considered as displacement. Than the conditions are complacent to satisfy. Only then the water depth and the velocity are measured in different location.
7. Important characteristic for testing are the components that are dumped into partial water flow. The procedure the real life practice.

3.7 Observations

During the experiments, the following observations were made:

i) The water surface downstream of the test section was slightly lower than the upstream section.
ii) The velocity over the apron was higher than that of downs tream and approach velocity was less than downstream velocity.
iii) The larger the size of the protection element greater velocity required to cause incipient condition.
iv) The velocity at the center was greater than that of both bank side.
v) As the velocity was increased the protection elements started vibrating.
vi) For geobags, group movement or sliding was observed while blocks moved individually.
vii) Square shaped bags required higher velocity to reach incipient condition than that of rectangular bags.

Photographs 3.7 to 3.9 show the various experimentations in the laboratory.

Photograph 3.7: Side view of the apron after dumping of CC blocks.

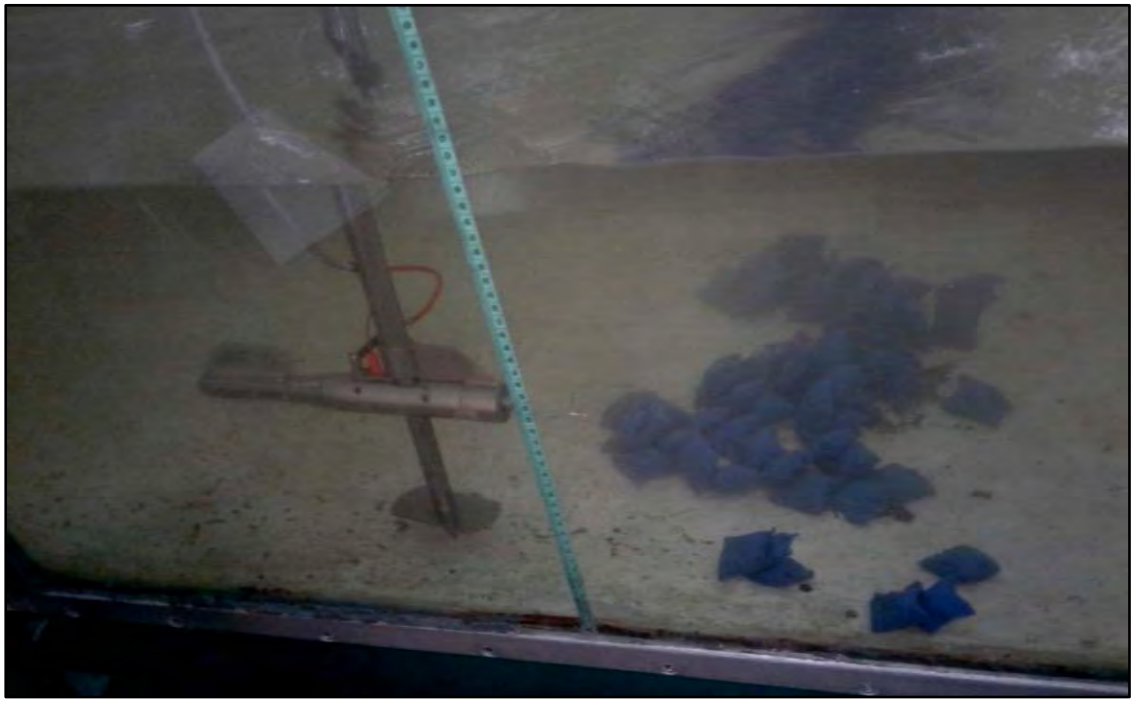

Photograph 3.8: Measurement of incipient velocity for geobags.

Photograph 3.9: Dumping of CC block to construct apron in the flume.

CHAPTER FOUR

RESULTS AND DISCUSSIONS

4.1 Introduction

Laboratory experiments have been conducted to investigating the behavior of toe protection elements (e.g. CC blocks and geobags) of river bank protection works. At fast, the placement of different types of protection element was observed. Incipient condition of CC blocks and geobags are described in this chapter. These results are then utilized to study the incipient condition of the elements when they are dumped in the flowing water. The later parts of this chapter explain the incipient behavior of the blocks and geobags when they provide a protection layer over the channel bed.

4.2 Results of Incipient Motion

Vibration of bed-material particles is an indication that movement is about to begin. This indicates the response of particles to the passing flow, which causes pressure differences and shear stresses that lead to lift and drag forces. If these forces increase over time, the in-place vibration may change to motion. The CC block traveled relatively less distance than geobag during the course of its settling.

Two setup were investigated for both block and geobag during the eighteen experimental run to observe the incipient condition of different types of protection elements. A power regression analysis of the experimental data has been performed. In the following sections the results of experiments for block and geobag are presented.

4.3 Results for CC Block

Data are collected during the experimental runs and shown in tabular form in Appendix B (Run 1 to Run 6). Six experimental runs have been conducted in this phase.

Table 4.1: Results of incipient motion experiments for CC block

Setup	Size of Block, d(m)	Initial Depth of flow, h(m)	Depth of flow, h(m)	Velocity (m/s)	d/h	$V/\sqrt{(\Delta_b gh)}$
S1	0.023	0.25	0.38	0.709	0.060	0.367
	0.021	0.23	0.375	0.752	0.056	0.392
	0.016	0.315	0.505	0.523	0.031	0.235
S2	0.023	0.18	0.295	0.762	0.077	0.447
	0.021	0.25	0.4	0.740	0.052	0.373
	0.016	0.33	0.47	0.569	0.034	0.265

Table 4.1 shows the parameter values of the tests for CC block where Δ_b=1, (relative submerged unit weight of CC block). Two setups for three types of block are conducted. On the basis of expression of incipient motion as shown in equation (2.13), a power regression analysis of the experimental data has been performed resulting:

$$\frac{d}{h} = 0.217\left(\frac{V}{\sqrt{\Delta_b gh}}\right)^{1.363} \qquad (4.1)$$

Equation (4.1) can be used to determine the CC block size to be used in toe protection when other parameters are known. Figure 4.1 shows the plot of equation (4.1). The coefficient of determination (R^2) for this equation is 0.951 which may be considered satisfactory.

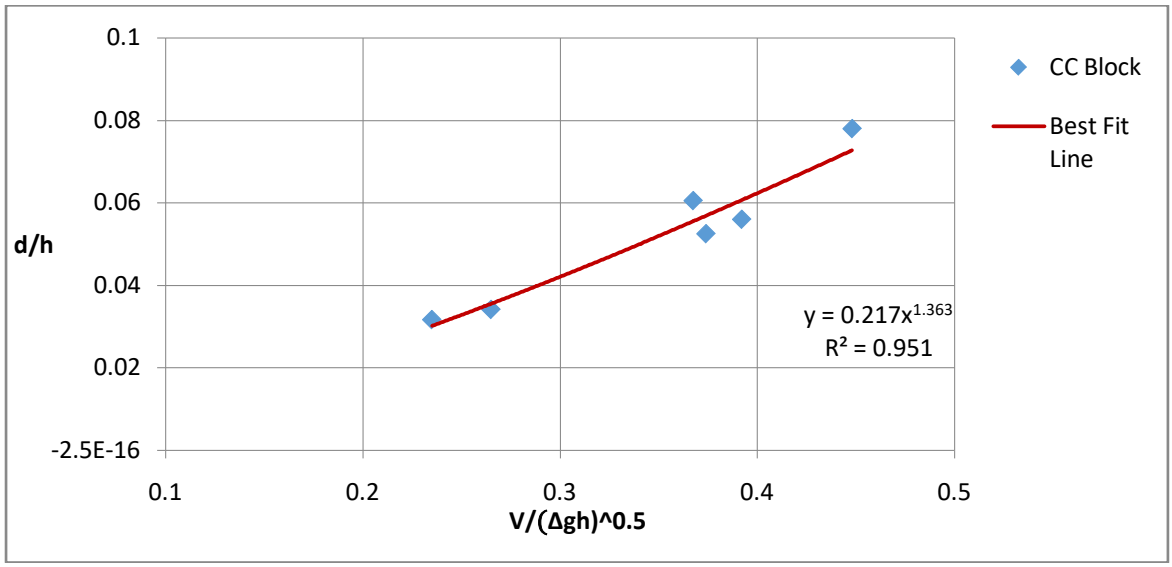

Figure 4.1: Plot of *d/h* against $V/\sqrt{(\Delta_b gh)}$ for CC block**.**

4.4 Results for hand placed CC Block

In this case the CC blocks are placed by hand, one by one while the water was flowing at very low flow (50 m^3/h). The intention of conducting the experiment in this manner is to investigate the probable influence of dumping/placement that may affect incipient condition/velocity. Data are collected during the experimental runs and shown in tabular form in Appendix B (Run 7 and Run 8). Two experimental runs have been conducted in this phase. The data are shown below.

Table 4.2: Results of incipient motion experiments for CC block
(Two layer CC 16 mm Block).

Set up	Size of Block, d (m)	Initial Depth of flow, hi (m)	Depth of flow, h (m)	Velocity (m/s)	d/h	$V/\sqrt{(\Delta_b gh)}$
S1	0.016	0.25	0.38	0.661	0.042	0.342
S2	0.016	0.28	0.4	0.672	0.040	0.339

Table 4.2 shows the parameter values of the tests for CC block. Two setups for 16 mm block are conducted. On the basis of expression of incipient motion as shown in equation (2.13), a power regression analysis of the experimental data has been performed resulting:

$$d/h = 0.483\left(\frac{V}{\sqrt{\Delta_b\, gh}}\right)^{2.25} \qquad (4.2)$$

Equation (4.2) can be used to determine the CC block size to be used in toe protection when other parameters are known. Figure 4.2 shows the plot of equation (4.2). The coefficient of determination (R^2) for this equation is 0.872 which may be considered as satisfactory.

Therefore, it may be considered that dumping of cc block above water surface and hand placing of cc block on the flume bed is likely to behave the same at the time of incipient condition.

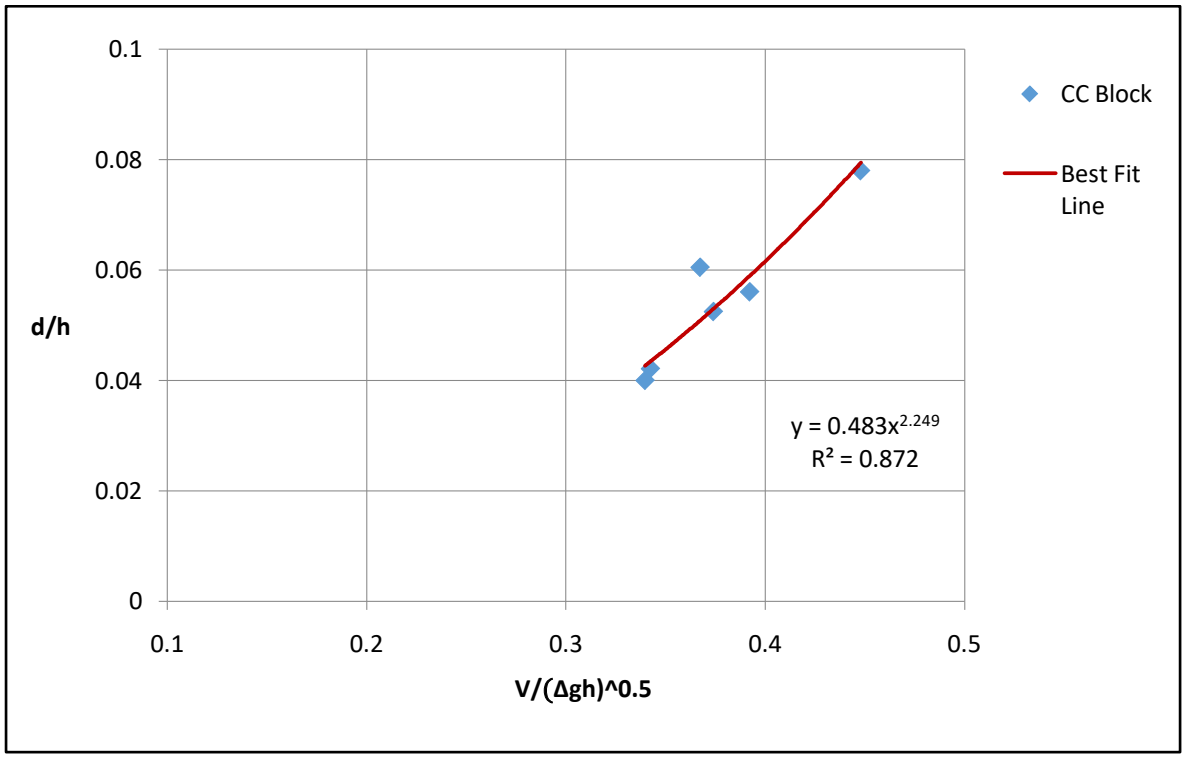

Figure 4.2: Plot of *d/h* against $V/\sqrt{(\Delta_b gh)}$ for CC (Two layer CC 16mmBlock).

4.5 Results for Geobag

Data are collected during the experimental runs and shown in tabular form in Appendix B (Run 9 to Run 18). Ten experimental runs have been conducted in this phase.

Table 4.3: Results of incipient motion experiments for geobag

Setup	Size of bag, *d*(m)	Initial Depth of flow, *h*(m)	Depth of flow, *h*(m)	Velocity, *V*(m/s)	*d/h*	$V/\sqrt{(\Delta_g gh)}$
S1	0.025	0.25	0.37	0.661	0.068	0.347
	0.025	0.25	0.35	0.579	0.074	0.312
	0.023	0.25	0.43	0.646	0.055	0.314
	0.024	0.25	0.41	0.629	0.059	0.314
	0.020	0.25	0.36	0.662	0.057	0.352
S2	0.025	0.3	0.43	0.588	0.059	0.286
	0.025	0.3	0.435	0.610	0.059	0.295
	0.023	0.3	0.45	0.629	0.052	0.299
	0.024	0.3	0.4	0.629	0.061	0.318
	0.020	0.3	0.425	0.557	0.048	0.272

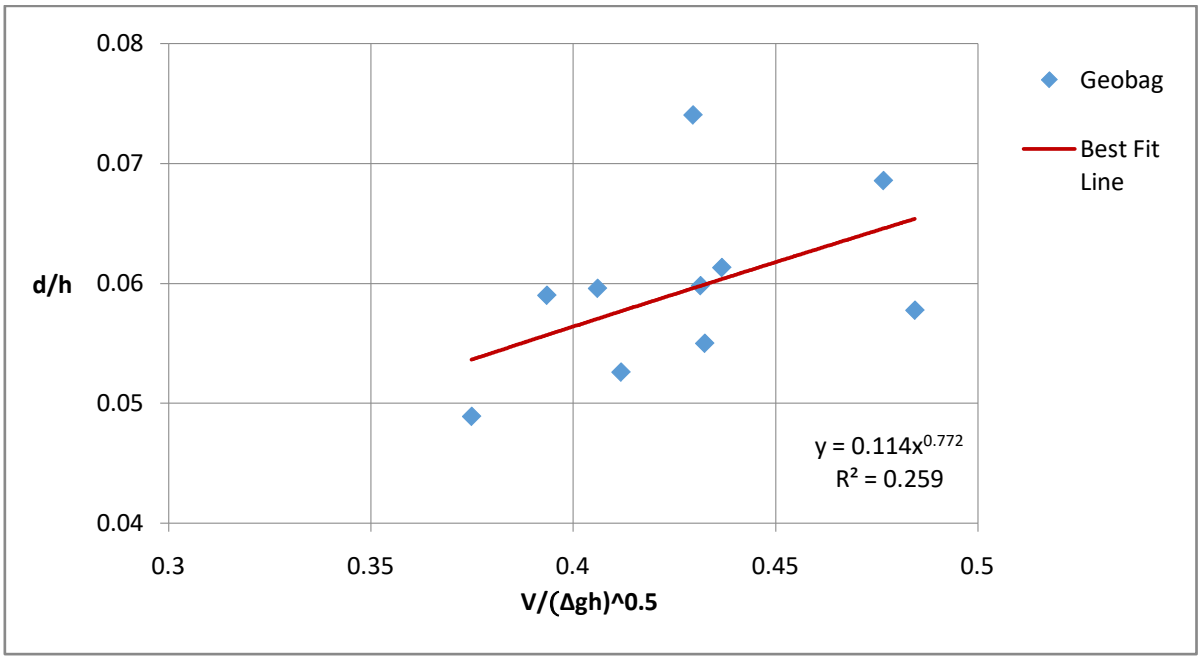

Figure 4.3: Plot of *d/h* against $V/\sqrt{(\Delta_g gh)}$ for geobag

Table 4.3 shows the parameters of the tests for geobag where Δ_g(relative submerged unit weight of geobag) = 0.53. Two setups for five types of geobag are conducted. On the basis of expression of incipient motion as shown in equation (2.13), a power regression analysis of the experimental data has been performed resulting:

$$d/h = 0.114\left(\frac{V}{\sqrt{\Delta_g gh}}\right)^{0.772} \quad (4.3)$$

Equation (4.3) can be used to determine the size of geobag to be used in toe protection when other parameters are known. Figure 4.3 shows the plot of equation (4.3). The coefficient of determination (R^2) for this equation is 0.259.

4.6 CC Block and Geobag

On the basis of expression of incipient condition as shown in equation (2.13) a power regression analysis using both (CC block and geobag) experimental data has been performed as shown in Figure 4.4, resulting:

$$d/h = 0.154\left(\frac{V}{\sqrt{\Delta gh}}\right)^{1.092} \quad (4.4)$$

Equation (4.4) can be used to determine the size of block and geobag to be used in toe protection when other parameters are known. Here Δ can be considered as either, Δ_b =1 or Δ_g= 0.53. The coefficient of determination (R^2) for this equation is 0.794. Also, it is needless to mention that equation (4.1) and (4.3) is better for CC block and geobag, respectively.

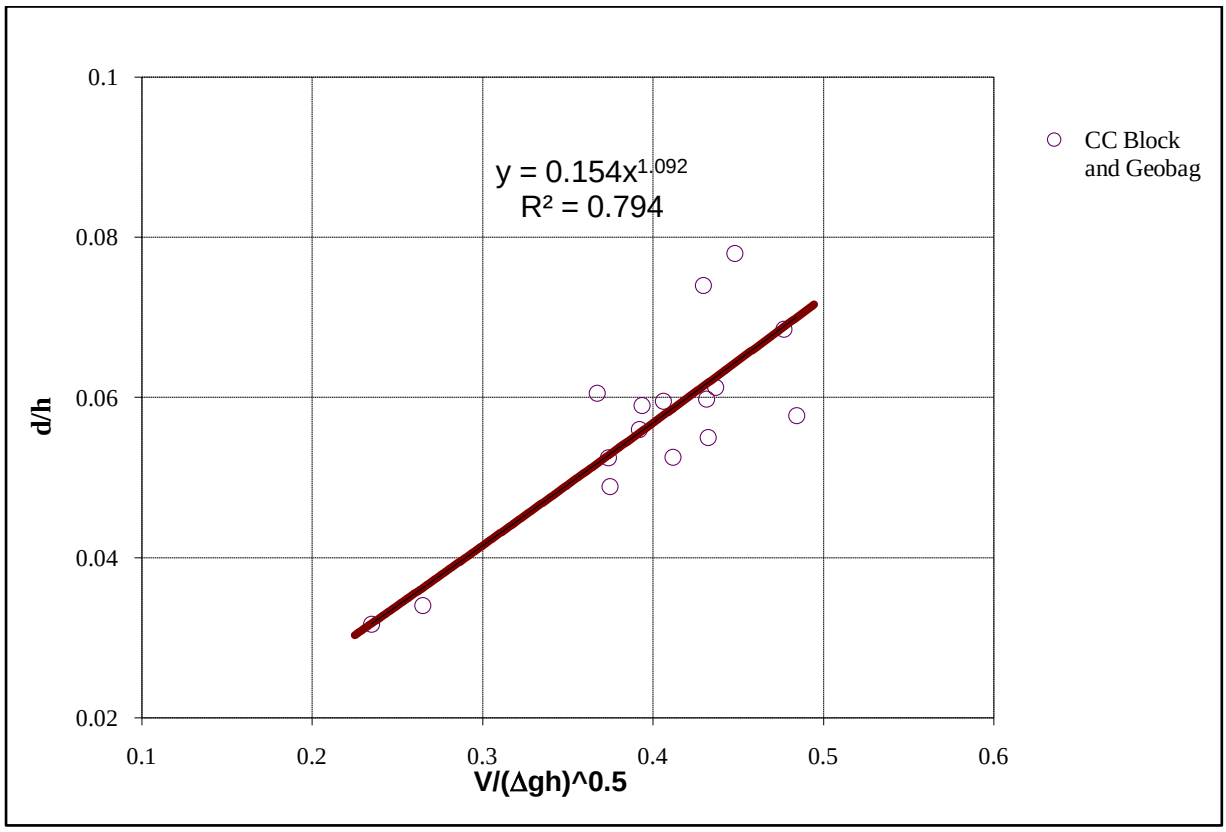

Figure 4.4: Plot of *d/h* against $V/\sqrt{(\Delta gh)}$ for both geobag and CC block.

4.7 Analysis of current and previous study data for CC Block

Figure 4.5 shows the plot considering the current data and previous study (Raju, 2011) data for CC block where the experimental setup and the protection elements were similar but with different hydraulic parameters.

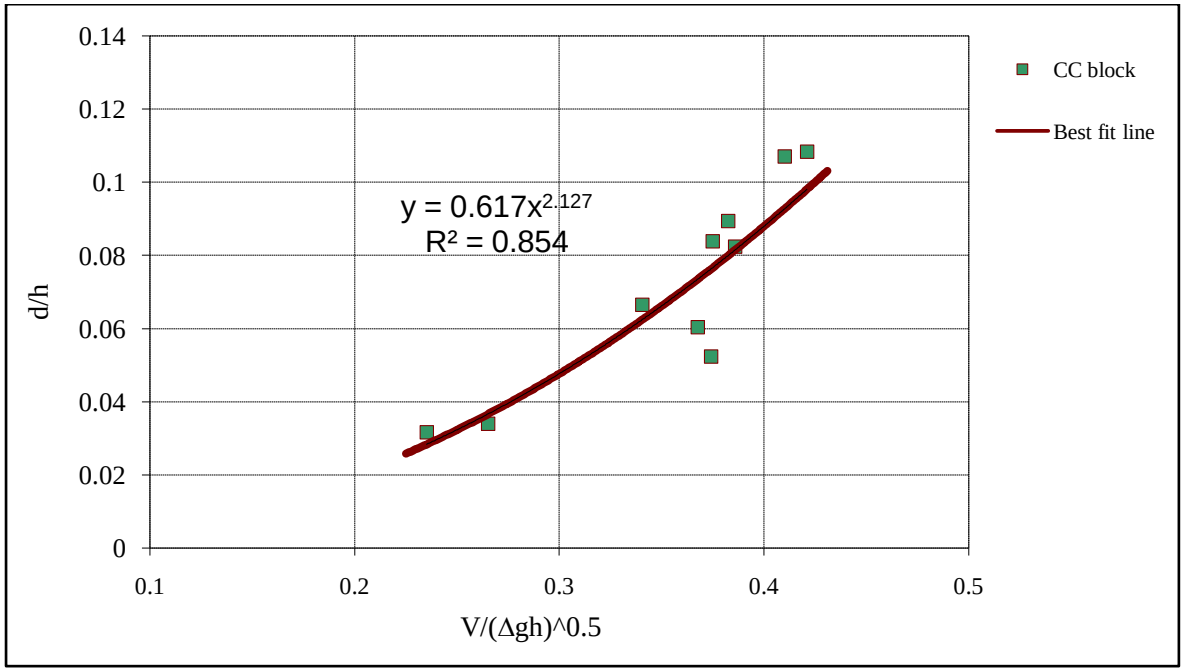

Figure 4.5: Plot of d/h against $V/\sqrt{(\Delta_b gh)}$ for CC block (Current and previous data).

A power regression analysis of the experimental data has been performed resulting:

$$d/h = 0.617\left(\frac{v}{\sqrt{\Delta_b gh}}\right)^{2.127} \quad (4.5)$$

Equation (4.5) can be used to determine the CC block size to be used in toe protection when other parameters are known. The coefficient of determination (R^2) for this equation is 0.854 (Power) which may be considered satisfactory.

4.8 Analysis of current and previous study data for Geobag

Figure 4.6 shows the data of current and previous study (Raju, 2011) for geobags.

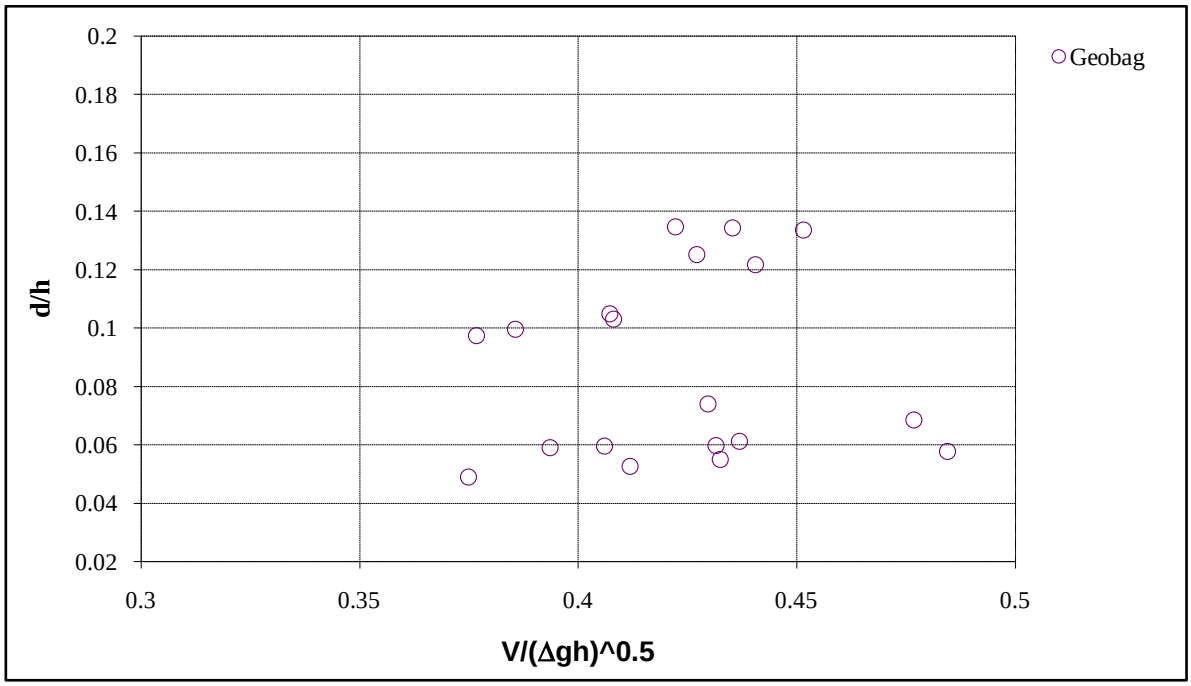

Figure 4.6: Plot of *d/ h* against $V/\sqrt{(\Delta_g gh)}$ for geobag (Current and previous data)

4.9 Analysis of current and previous study data for CC block and Geobag

Figure 4.7 shows the plot considering the current and previous study (Raju, 2011) data for cc block and geobags.

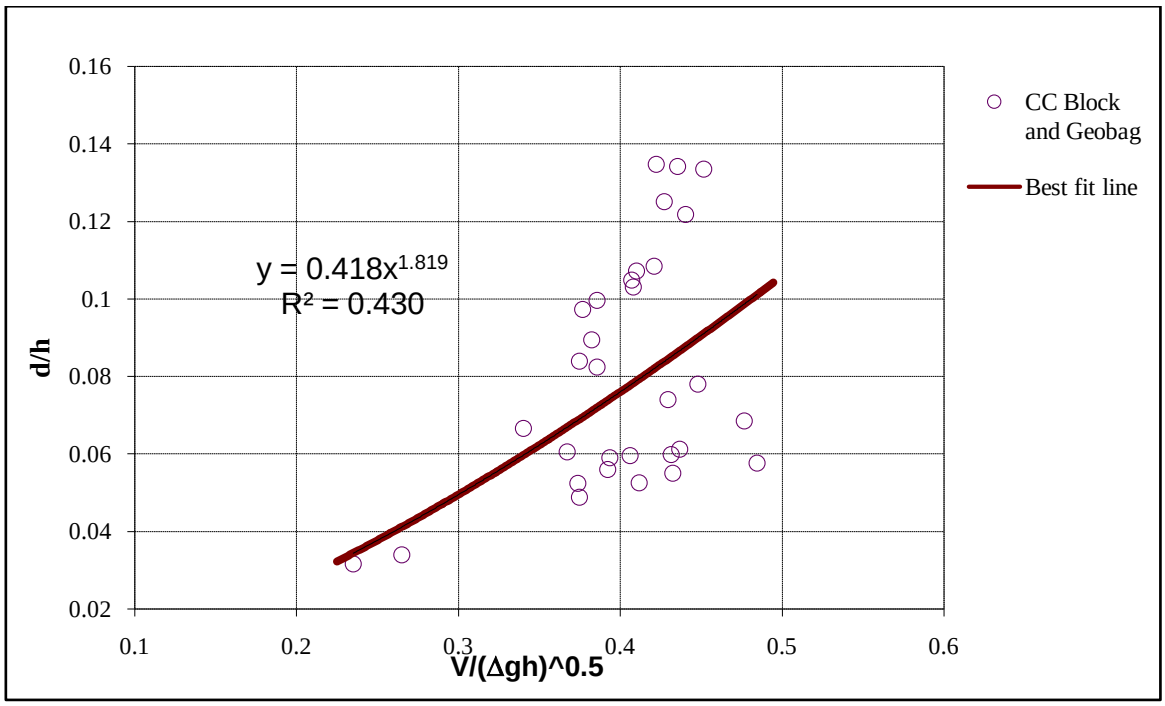

Figure 4.7: Plot of *d/h* against $V/\sqrt{(\Delta gh)}$ for CC block and geobag (Current and previous data)

On the basis of expression of incipient motion as shown in equation (2.13), a power regression analysis of the experimental data has been performed resulting:

$$d/h = 0.42\left(\frac{V}{\sqrt{\Delta gh}}\right)^{1.82} \quad (4.6)$$

Equation (4.6) can be used to determine the size of geobag to be used in toe protection when other parameters are known. The coefficient of determination (R^2) for this equation is 0.43.

4.10 Graphical expression for interaction among the parameters

Equation (4.5) is used to develop the nomograph shown in Figure 4.8, which is applicable to a cc block weighing 2000 kg/m^3. It is seen that the trend of the curves at higher depth are towards right. This implies that for a given block size it can withstand higher velocity at higher depth. For given flow depth and depth averaged velocity, the required thickness of protection using CC block can be selected from this graph.

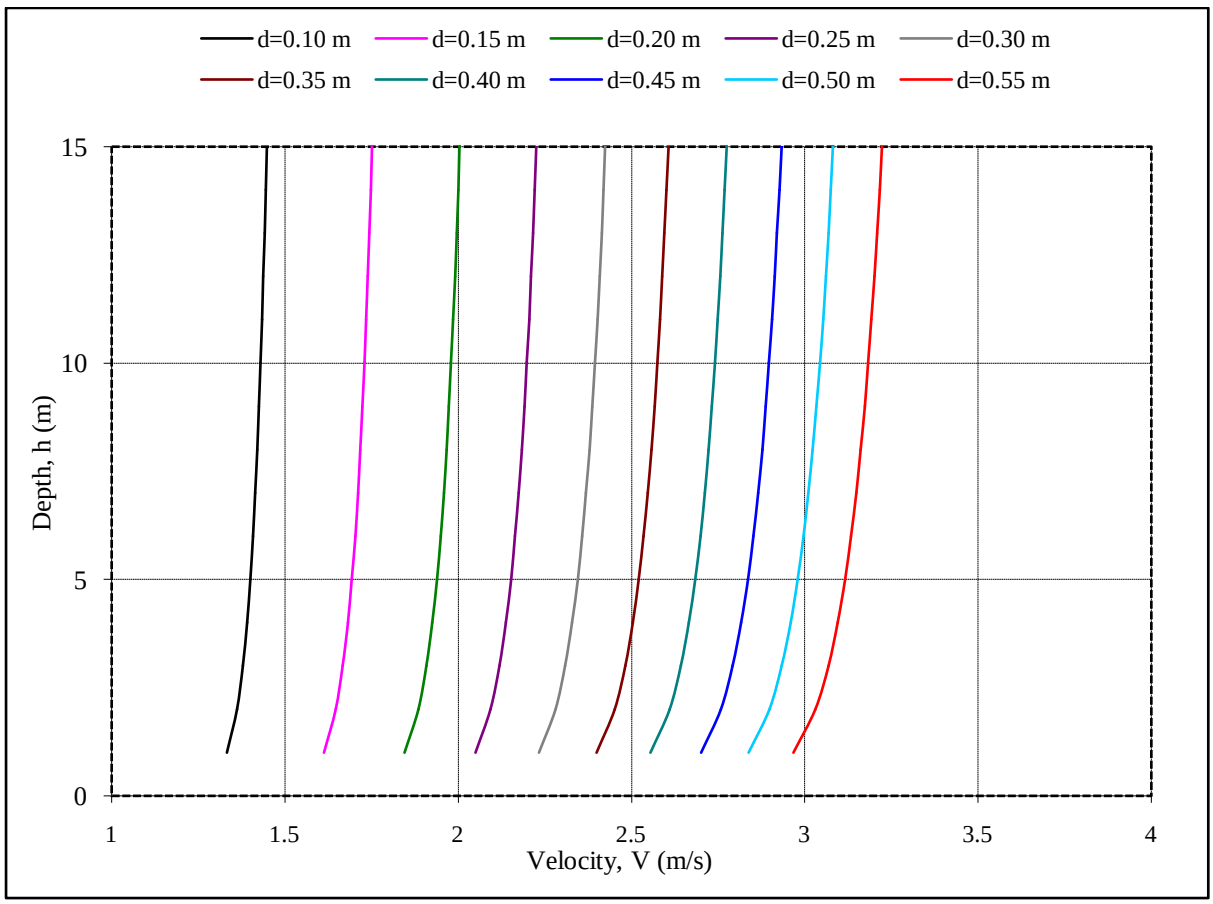

Figure 4.8: Plot of depth versus depth average incipient velocity for CC block.

4.11 Comparison among the formula for incipient motion of CC block

Figure 4.9 shows, the plot of equation 4.5, a comparison among the obtained relationship and relationship given by Maynord (1989), Neil (1967) and Inglis (1921). Here ρ_s=2000 kg/m^3, ρ_w=1000 kg/m^3, and $V = 3.5\ m/s$.

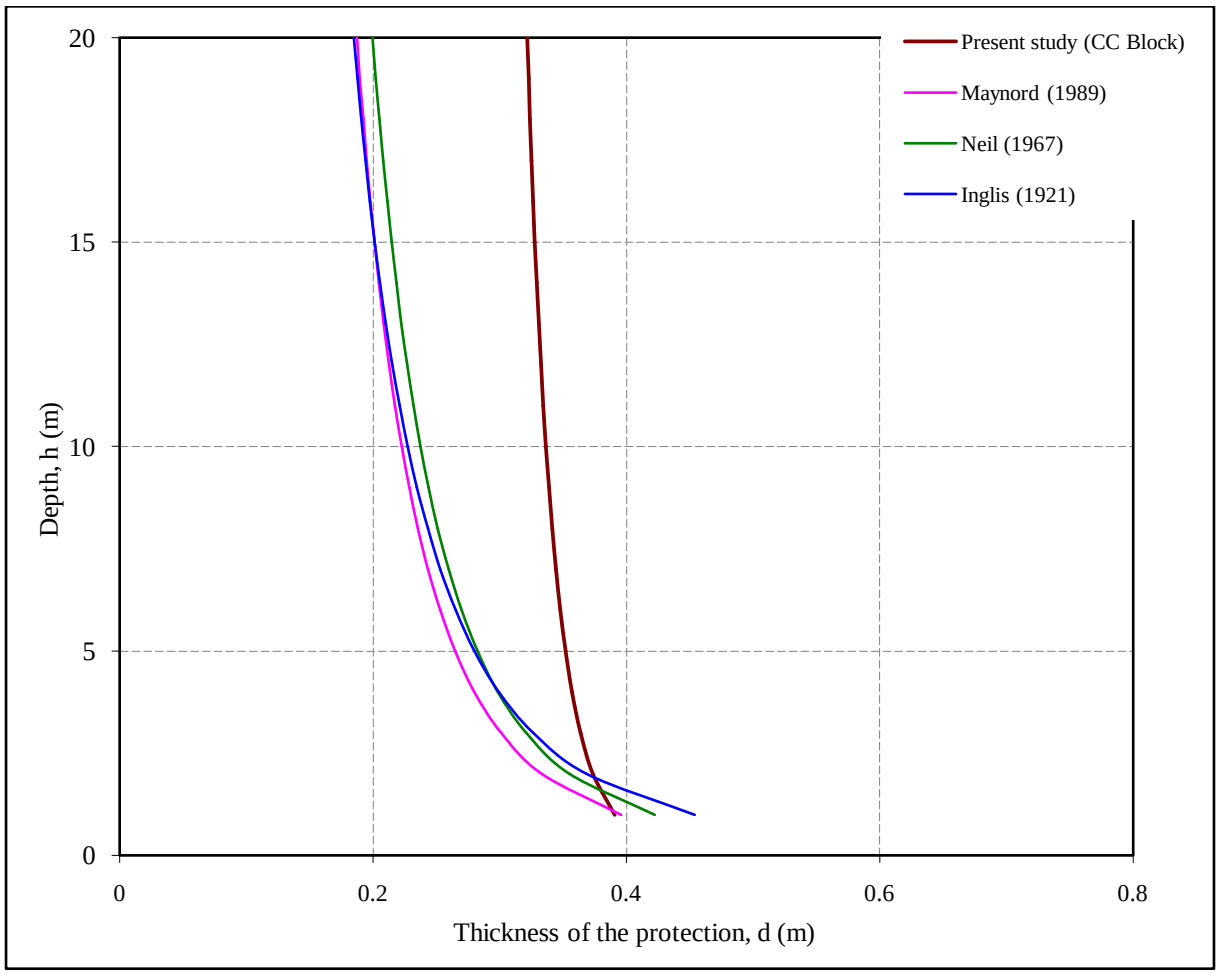

Figure 4.9 Comparison among incipient motion formula on the basis of depth versus thickness of protection for prototype condition.

The present study finds that requirement of protection thickness is more than other equations. This is quite similar to Raju (2011). The possible reason for the deviation from other formulae is believed to be the definition of incipient motion and the difference in experimental setup in those studies. Current study considers incipient motion to be the first movement of any protection unit. On the other way, it may be stated that the proposed relationships show indication to selection of larger protection unit (CC block) than the available / conventional formula.

4.12 Comparison among the formula for incipient motion of CC block and geobag.

Figure 4.10 shows, a comparison between the obtained relationship for CC block and geobag, Here Δ_b = 1, Δ_g = 0.53 and V = 3.5 m/s, In this figure the curve for CC block is obtained from equation 4.5. However, the following equation is used for geobag since the relationship obtained from the previous study is better than the current one:

$$d/h = 0.64\left(\frac{V}{\sqrt{\Delta_g gh}}\right)^{1.95} \quad (4.7)$$

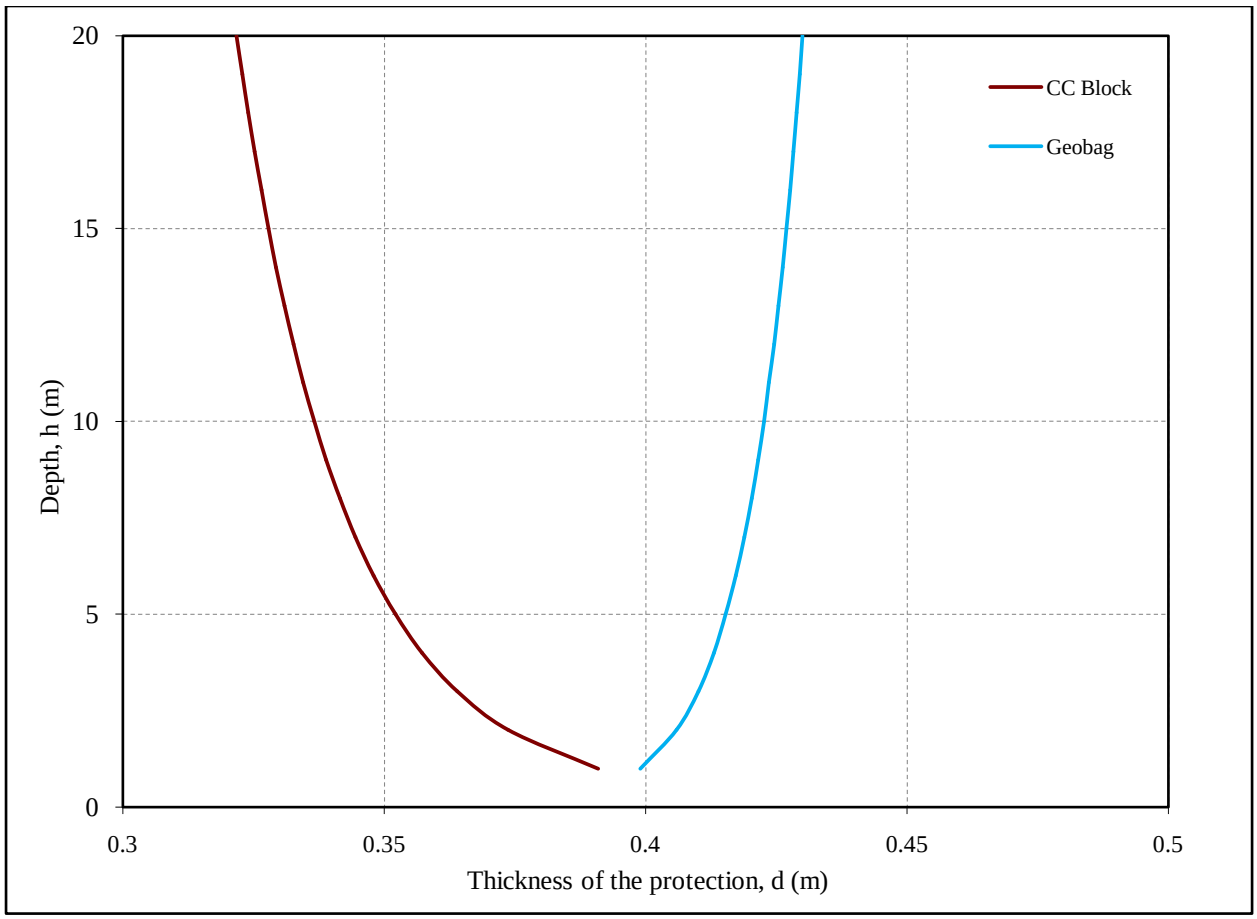

Figure 4.10 Comparison among incipient motion formula on the basis of depth versus thickness of protection for prototype condition.

It is observed from the figure that higher protection thickness is required for geobag than the CC block. This discrepancy may be due to the fact that the geobags are relatively flat and less dense, and thus their underwater functional behavior becomes more composite as a group. Moreover it is observed during the experimentation that at the moment of incipient condition, CC block moved individually but geobags moved collectively (in a group of 2~4 no.). Also, the specific gravity of geobag is almost half of the CC block.

CHAPTER FIVE

CONCLUSIONS AND RECOMMENDATIONS

5.1 Introduction

The experimental study of incipient condition of toe protection elements incipient condition has been conducted. Relationships for governing parameters of the incipient velocity of toe protection elements have been theoretically analyzed. These relationships are then verified using laboratory data. A total of two types of elements (CC block and geobag) consisting of three sizes of CC blocks and five different sizes of geobags have been used to conduct experiments. In this chapter, the conclusions and recommendations are made.

5.2 Conclusions

Based on the experimental investigations carried out in the present study, the following conclusions are made:

i) Owing to the variation in sizes and their positioning in different directions, incipient motion of does not occur at one time. When the CC block or geobag starts vibrating then movement is initiated and it is considered here that incipient condition has been achieved.

ii) A total of eighteen experimental run consisting of five different sizes (ranging from 20mm-24mm) of geobags and three different sizes (ranging from 16mm-23mm) of CC blocks have been to conducted for discharges varying from 0.066 m^3/s to 0.187 m^3/s.

iii) An empirical relationship (equation 4.1) to determine the size of CC block as toe protection element based on incipient condition is developed with a coefficient of correlation (R^2) is 0.951. Also, an empirical relationship (equation 4.3) to determine the size of geobag as toe protection element based on incipient condition is developed with a coefficient of correlation (R^2) is 0.53.

iv) Improved empirical relationship is found when both current and previous data are taken into account.

v) For incipient condition, CC blocks can withstand at higher velocity at higher depths (Figure 4.8).

vi) Proposed relationships show indication to selection of larger protection unit than the conventional formula (Figure 4.9).

vii) It is found from the study that for a given velocity the required thickness of protection decreases with the increase of depth of flow for CC block. However, reverse condition is observed

for geobag (Figure 4.10). This discrepancy may be due to the fact that the geobags are relatively flat and less dense, and thus their underwater functional behavior becomes more composite as a group. Also, the specific gravity of geobag is almost half of the CC block.

viii) Finally, it is expected that the outcome of the present study can be taken as a tentative guideline for selection of protection elements for river bank toe protection works.

5.3 Recommendations for future study

Following recommendations are suggested for further study:

i) Morphological response of the river bed due to random placement of toe protection elements during construction can be investigated.
ii) Future research may be undertaken to investigate hydraulic behavior around an apron of transverse type river training structures.
iii) Similar study may be undertaken in physical modeling facility considering live bed condition.

REFERENCES

1.1. References:

Abt, S. R. and Johnson, T. L. (1991), "Riprap design for overtopping flow."J. Hydraul Eng,,117(8), 959-972.

Ahmed, T. (2014). "An experimental study on placement of toe protection element of river bank protection works under live bed condition". M. Sc. Engg. Thesis, Department of Water Resources Engineering, BUET, Dhaka 1000, Bangladesh.

Anisur, R. (2010). "An experimental study on comparatively analysis of Design and performance of Bank protection works of jamuna river at titporal and debdanga". M. Engg. Thesis, Department of Water Resources Engineering, BUET, Dhaka 1000, Bangladesh.

Beheshti, A. A., and Ashtiani, B. A(2008). "Analysis of threshold and incipient conditions for sediment movement". *J. Coastal Eng.,* Elsevier, 55, 423-430.

Bettess, R. (1984). "Initiation of sediment transport in gravel streams." Proceedings of the Institution of Civil Engineers, Technical Note 407, Part 2.

Blench, T. (1966). Discussion on "Sediment transport mechanics: initiation of motion." J. Hydraulics Div., ASCE, 92(HY5), 287-288.

Bogardi, J. L. (1978). "Sediment transport in alluvial streams." Akademiai Kiado, Budapest.

Brahms, A. (1753). "Anfangsgründe der deich-und." Wasserbaukunst, Aurich (Source: Van Rijn, 1993).

Buffington, J. M. (1999) "The legend of A.F. Shields."*J. Hydraul. Eng* , 125 (4), 376-387.

BWDB, (2010). "Guidelines for river bank protection", prepared for Bangladesh Water Development Board under Jamuna-Meghna River Erosion Mitigation Project, Government of the People's Republic of Bangladesh.

Chepil , W. S. (1945) "Dynamics of Wind Erosion: II, Initiation of Soil Movement," Soil Science, Vol, 60, PP. 397-411.

FAP 21/22 (1993). Main Report on Bank Protection; FAP 21; Volume 1A: Bank Protection and River Training (AFPM); Pilot Project; FAP 21/22; Final Report, Planning Study; Consulting Consortium, RHEIN-RUHR ING. GES. MBH, Dortmund, Germany.

Göğüş, M., and Defne, Z. (2005). "Effect of shape on incipient motion of large solitary particles". J. Hydraul. Eng. Div, ASCE, 131 (1), 38-45.

Halcrow and Associates, (2002). “Feasibility Study - Final Report”, Jamuna-Meghna River Erosion Mitigation Project, Volume 1 (Phase II), Main Report, Prepared for Bangladesh Water Development Board, Government of the People’s Republic of Bangladesh.

Haque, M. E. (2010). “An experimental study on flow behavior around launching apron”. M.Sc. Thesis, Department of Water Resources Engineering, BUET, Dhaka.

Hartung, F. and Scheuerlein , H. (1970), “Design of overflow rockfill dams,”10th ICOLD –Congress, Vol,1, Q.36,R.35.

Ikeda, S, and Miyashita, S, (1981), “On Sand Movement on Slopes,” Proceedings of Japanese conference on Hydraulics, Japan Society of Civil Engineers, Vol, 25,1981, pp, 55-60 (in Japanese).

Inglis, C. C. (1949), “The behavior and control of rivers and canals (with the aid of models)”, Part II. Central Waterpower Irrigation and Navigation Research Station, Poona, India.

Lavelle, J.W. and Mofjed, H, O, (1987). “Do critical stresses for incipient motion and erosion really exist J Hydraul,” Eng,113(3)370. 385.

Lick, W., Jin, L., and Gailani, J. (2004). “ Initiation of movement of quartz particles”. *J. Hydraul. Eng.*, ASCE, 130 (8), 755-761.

Ling, C. H. (1995), “Criteria for incipient motion of spherical sediment particles”. *J. Hydraul. Eng.*, ASCE, 121 (6), 472-478.

Maynord, S. T., Ruff, J. F. and Abt, S. R. (1948). “Riprap Design”. *J. Hydraul. Eng.*, ASCE, 115 (7), 937-949.

Meyer-Peter, E., and Muller, R. “Formulas for bed load transport.” International Association for Hydraulic Structures Research, Second Meeting, Stockholm, Appendix 2, 39-64.

Rabiqul, M. M. (2003). “An experimental study on Local scour at the toe protection element”. M. Engg. Thesis, Department of Water Resources Engineering, BUET, Dhaka 1000, Bangladesh.

Neill, C. R. , (1967). “Mean velocity criterion for scour of coarse uniform bed material”. Proceedings 12th Congress, International Association for Hydraulic Research, Vol. 3.

.Northwest Hydraulic Consultants. (2006) “Physical Model Study”, Final Report. Prepared for Jamuna-Meghna River Erosion Mitigation Project. Bangladesh Water Development Board, Ministry of Water Resources, Government of Bangladesh.

Onl, N. E. (1996). “Initiation of motion of coarse particles on a slope by regular waves” . PhD thesis, Istanbul Technical University, Istanbul, Turkey (in Turkish).

Peirson, W. L. and Cameron, S,(2006), “Design of rock protection for prevention of erosion by water flows down steep inclined slopes.”*J Hydraul. Eng.,* 132(10), 1110-1114.

Pilarczyk, K. W. (1995). “Novel systems in coastal engineering; geotextile systems and other methods, an over view.” Rijkswaterstaat, Delft, the Netherlands.

Pilarczyk, K. W. (2000). “Geosynthetics and geosystems in hydraulic and coastal engineering”, Balkema, Rotterdam, The Netherlands.

Przedwojski, B., Błażejewski, R. and Pilarczyk, K. W. (1995). “River training techniques: fundamentals, design and applications”. A. A. Balkema, Rotterdam, The Netherlands.

Raju, K. M. A. H. (2011). “An experimental study on settling behavior of toe protection elements of river bank protection works”. M.Sc. Engg. Thesis, Department of Water Resources Engineering, BUET, Dhaka 1000, Bangladesh.

Restall, S. J., Jackson, L. A., Heerten, G., and Hornsey, W. P. (2002). “Case studies showing the growth and development of geotextile sand containers: an Australian perspective”. *J. Geotextiles and Geomembranes*, Elsevier, 20 (2002), 321-342.

RRI (2010). River Research Institute. “Additional test to carryout investigation regarding performance of falling apron, drop test for dumping of geobag and outflanking problem by physical model to address bank erosion of Bangladesh”. Prepared for Bangladesh Water Development Board.

Scheuerlein, H. (1968). “Der rauhgerinneabfluss, Bericht Nr”.14 der versuehsanstalt fur Wasserban der Technischen Universitat Miinchen. Herausgegeben von F.Hartun, Miinchen/Obermach 1968 (in German).

Stevens, M. A., and Oberhagemann, K. (2006). “Geobag revetments.” Special Report 17 of Jamuna-Meghna River Erosion Mitigation Project, Prepared for Bangladesh Water Development Board, Government of the People’s Republic of Bangladesh.

Smith, D. A., and Cheung, K. F. 2004. “Initiation of motion of calcareous sand”. *J. Hydraul. Eng.*, ASCE, 130 (5), 467-472.

Ünal, N. E., and Bayazit, M. (1998). “Incipient motion of coarse particles on a slope by regular or irregular waves”. J. Waterw., Port, Coastal, Ocean Eng.,ASCE, 124 (1), 32-35.

USACE. (1994). “Hydraulic design of flood control channels”. U. S. Army Corps of Engineers, Manual EM 1110-2-1601.

Van Hijum, E, and Pilarczyk , K.W.(1982) . “ Equilibrium profile and longshore transport of coarse material under regular and irregular and irregular wave attac.” *Delft Hydr*. Pub.No.274, Delft, The Netherland.

Zaman, M. U., and Oberhagemann, K. (2006). Special Report 23: “Design brief for river bank protection implemented under JMREMP.” Prepared for Jamuna-Meghna River Erosion Mitigamation Project. Bangladesh Water Development Board. Ministry of Water Resources, Government of Bangladesh.

Zhu, L.,Wang, J., Cheng, N-S., Ying, Q., and Zhang, D.(2004), “Settling distance and incipient motion of sandbags in open channel flows”. *J. Waterw., Port, Coastal, Ocean Eng.,*ASCE, 130 (2), 98-103.

APPENDIX – A

Sample Calculation to Determine Experimental Size of CC Block

(i) Let,

ū = 3.3 m/s

h = 10 m and

D_n = 0.4 m.

Then, $K_h = \left({}^{h}/_{D_n} + 1\right)^{-0.2}$

= 0.52

Now from equation (3.1) and other values mentioned above results in

D_n = 451 mm ≈ 460 mm.

For present study, D_n = 460/20 = 23 mm that is block type 'D1a' of Table 3.2. (ii) Let,

ū = 3.1 m/s

h = 9 m and

D_n = 0.4 m.

Then, $K_h = \left({}^{h}/_{D_n} + 1\right)^{-0.2}$

= 0.53

Now from equation (3.1) and other values mentioned above results in

D_n = 405 mm ≈ 420 mm.

For present study, D_n = 420/20 = 21 mm that is block type 'D2a' of Table 3.2.

(iii) Let,

ū = 2.8 m/s

h = 8 m and

D_n = 0.3 m.

Then, $K_h = \left({}^{h}/_{D_n} + 1\right)^{-0.2}$ = 0.51

Now from equation (3.1) and other values mentioned above results in D_n

= 318 mm ≈ 320 mm.

For present study, D_n = 320/20 = 16 mm that is block type 'D3a' of Table 3.2.

APPENDIX - B

Run 1:

CC Block=(20X20X20)mm,Date=22/12/17
Initial depth of flow=0 .23.m
Flume Width = 0.762m
Total Depth of Flow Y=0..375 m
Current meter constant, a= 0.1334

Initial water flow (Discharge)= 150 m3/h
Final water flow (Discharge)= 723 m3/h
Width of each strip, B/3 = 0 .254 m
b= 0.029

Location of Current meter		Current meter reading			Point Velocity V (m/s)
Horizontal	Vertical	Number of revolution N (rev).	Time of observation T (sec)	Revolution per second n (rev/see)	
At middle of first strip	at 0.2 Y	217	40.3	5.384	0.747
	at 0.6 Y	204	40.3	5.062	0.704
	at 0.8 Y	191	40.4	4.727	0.659
At middle of Second strip	at 0.2 Y	219	40.6	5.394	0.748
	at 0.6 Y	219	40.4	5.420	0.752
	at 0.8 Y	209	40.4	5.173	0.719
At middle of third strip	at 0.2 Y	224	40.5	5.530	0.766
	at 0.6 Y	225	40.4	5.569	0.771
	at 0.8 Y	213	40.4	5.272	0.732

Run 2:

CC Block= (23X23X23)mm, Date= 22/12/17
Initial depth of flow= 0.25m
Flume Width = 0.762m
Total Depth of Flow Y=0.38 m
Current meter constant, a= 0.1334
Initial water flow (Discharge)= 150 m3/h
Final water flow (Discharge)= 689 m3/h
Width of each strip, B/3 = 0.254 m
b= 0.029

Location of Current meter		Current meter reading			Point Velocity V (m/s)
Horizontal	Vertical	Number of revolution N (rev).	Time of observation T (sec)	Revolution per second n (rev/see)	
At middle of first strip	at 0.2 Y	201	40.4	4.975	0.692
	at 0.6 Y	187	40.4	4.628	0.646
	at 0.8 Y	171	40.4	4.232	0.593
At middle of Second strip	at 0.2 Y	206	40.4	5.099	0.709
	at 0.6 Y	205	40.2	5.099	0.709
	at 0.8 Y	193	40.1	4.812	0.671
At middle of third strip	at 0.2 Y	209	40.5	5.160	0.717
	at 0.6 Y	209	41	5.097	0.709
	at 0.8 Y	195	40.2	4.850	0.676

Run 3:

CC Block=(23X23X23)mm, Date=22/12/18
Initial water flow (Discharge)= 150 m3/h
Initial depth of flow= 0.18m
Final water flow (Discharge)= 566m3/h
Flume Width = 0.762m
Width of each strip, B/3 = 0.254 m
Total Depth of Flow Y=0.295 m
b= 0.029
Current meter constant, a= 0.1334

Location of Current meter		Current meter reading			Point Velocity V (m/s)
Horizontal	Vertical	Number of revolution N (rev).	Time of observation T (sec)	Revolution per second n (rev/see)	
At middle of first strip	at 0.2 Y	214	40.4	5.297	0.735
	at 0.6 Y	211	40.4	5.222	0.725
	at 0.8 Y	199	40.5	4.913	0.684
At middle of Second strip	at 0.2 Y	222	40.6	5.467	0.758
	at 0.6 Y	222	40.4	5.495	0.762
	at 0.8 Y	211	40.2	5.248	0.729
At middle of third strip	at 0.2 Y	225	40.4	5.569	0.771
	at 0.6 Y	225	40.4	5.569	0.771
	at 0.8 Y	208	40.4	5.148	0.715

Run 4:

CC Block=(20X20X20)mm, Date=05/1/18
Initial depth of flow= 0.25m
Flume Width = 0.762m
Total Depth of Flow Y=0.40 m
Current meter constant, a= 0.1334

Initial water flow (Discharge)= 150 m3/h
Final water flow (Discharge)= 782m3/h
Width of each strip, B/3 = 0.254 m
b= 0.029

Location of Current meter		Current meter reading			Point Velocity V (m/s)
Horizontal	Vertical	Number of revolution N (rev).	Time of observation T (sec)	Revolution per second n (rev/see)	
At middle of first strip	at 0.2 Y	213	40.5	5.259	0.730
	at 0.6 Y	166	40.4	4.108	0.577
	at 0.8 Y	188	40.5	4.641	0.648
At middle of Second strip	at 0.2 Y	215	40.2	5.348	0.742
	at 0.6 Y	215	40.3	5.334	0.740
	at 0.8 Y	200	40.2	4.975	0.692
At middle of third strip	at 0.2 Y	219	40.5	5.407	0.750
	at 0.6 Y	216	40.4	5.346	0.742
	at 0.8 Y	203	40.5	5.012	0.697

Run 5:

CC Block=(15X15X15)mm, Date=05/01/18

Initial water flow (Discharge)= 150 m3/h

Initial depth of flow=0 .33m

Final water flow (Discharge)=698 m3/h

Flume Width = 0.762m

Width of each strip, B/3 = 0.254 m

Total Depth of Flow Y=0.47 m

b= 0.029

Current meter constant, a= 0.1334

Location of Current meter		Current meter reading			Point Velocity V (m/s)
Horizontal	Vertical	Number of revolution N (rev).	Time of observation T (sec)	Revolution per second n (rev/see)	
At middle of first strip	at 0.2 Y	168	40.5	4.148	0.582
	at 0.6 Y	163	40.4	4.034	0.567
	at 0.8 Y	146	40.4	3.613	0.511
At middle of Second strip	at 0.2 Y	164	40.5	4.049	0.569
	at 0.6 Y	164	40.5	4.049	0.569
	at 0.8 Y	162	40.5	4	0.562
At middle of third strip	at 0.2 Y	162	40.4	4.009	0.563
	at 0.6 Y	165	40.4	4.084	0.573
	at 0.8 Y	162	40.5	4	0.562

Run 6:

CC Block =(15X15X15)mm, Date=15/12/17
Initial water flow (Discharge)= 150 m3/h
Initial depth of flow= 0.31m
Final water flow (Discharge)= m3/h
Flume Width = 0.762m
Width of each strip, B/3 = 0.254 m
Total Depth of Flow Y=0.50 m
b= 0.029
Current meter constant, a= 0.1334

Location of Current meter		Current meter reading			Point Velocity V (m/s)
Horizontal	Vertical	Number of revolution N (rev).	Time of observation T (sec)	Revolution per second n (rev/see)	
At middle of first strip	at 0.2 Y	143	40.4	3.539	0.501
	at 0.6 Y	148	40.4	3.663	0.517
	at 0.8 Y	139	40.5	3.432	0.486
At middle of Second strip	at 0.2 Y	147	40.8	3.602	0.509
	at 0.6 Y	150	40.5	3.703	0.523
	at 0.8 Y	145	40.4	3.589	0.507
At middle of third strip	at 0.2 Y	149	40.4	3.688	0.520
	at 0.6 Y	150	40.8	3.676	0.519
	at 0.8 Y	142	40.9	3.471	0.492

Run 7:

Two Layer CC Block.

CC Block =(15X15X15)mm, Date=19/05/17
Initial depth of flow= 0.25m
Flume Width = 0.762m
Total Depth of Flow Y=0.38 m
Current meter constant, a= 0.1334

Initial water flow (Discharge)= 150 m3/h
Final water flow (Discharge)= 630 m3/h
Width of each strip, B/3 = 0.254 m
b= 0.029

Location of Current meter		Current meter reading			Point Velocity V (m/s)
Horizontal	Vertical	Number of revolution N (rev).	Time of observation T (sec)	Revolution per second n (rev/see)	
At middle of first strip	at 0.2 Y	181	40.4	4.480	0.626
	at 0.6 Y	181	40.5	4.469	0.625
	at 0.8 Y	163	40.3	4.044	0.568
At middle of Second strip	at 0.2 Y	190	40.1	4.738	0.661
	at 0.6 Y	192	40.5	4.740	0.661
	at 0.8 Y	180	40.3	4.466	0.624
At middle of third strip	at 0.2 Y	193	40.4	4.777	0.666
	at 0.6 Y	191	40.8	4.681	0.653
	at 0.8 Y	185	40.4	4.579	0.639

Run 8:

Two Layer CC Block.

CC Block =(15X15X15)mm, Date=19/05/17
Initial depth of flow= 0.28m
Flume Width = 0.762m
Total Depth of Flow Y=0.40 m
Current meter constant, a= 0.1334
Initial water flow (Discharge)= 150 m3/h
Final water flow (Discharge)= 685 m3/h
Width of each strip, B/3 = 0.254 m
b= 0.029

Location of Current meter		Current meter reading			Point Velocity V (m/s)
Horizontal	Vertical	Number of revolution N (rev).	Time of observation T (sec)	Revolution per second n (rev/see)	
At middle of first strip	at 0.2 Y	193	40.5	4.765	0.664
	at 0.6 Y	182	40.3	4.516	0.631
	at 0.8 Y	172	40.2	4.278	0.599
At middle of Second strip	at 0.2 Y	197	40.4	4.876	0.679
	at 0.6 Y	195	40.4	4.826	0.672
	at 0.8 Y	185	40.1	4.613	0.644
At middle of third strip	at 0.2 Y	197	40.3	4.888	0.681
	at 0.6 Y	197	40.1	4.912	0.684
	at 0.8 Y	194	40.6	4.778	0.666

Run 9:

Date=26/03/18
Geobag (Blue),B2,
Initial depth of flow= 0.30m
Flume Width=0.762m
Total Depth of Flow Y=0.40 m
Current meter constant, a= 0.1334

Initial water flow (Discharge)= 150 m3/h
Final water flow (Discharge)= 578 m3/h
Width of each strip, B/3 = 0.254 m
b= 0.029

Location of Current meter		Current meter reading			Point Velocity V (m/s)
Horizontal	Vertical	Number of revolution N (rev).	Time of observation T (sec)	Revolution per second n (rev/see)	
At middle of first strip	at 0.2 Y	154	40.1	3.840	0.541
	at 0.6 Y	146	40.6	3.596	0.508
	at 0.8 Y	135	40.6	3.325	0.472
At middle of Second strip	at 0.2 Y	157	40.5	3.876	0.546
	at 0.6 Y	159	40.4	3.935	0.554
	at 0.8 Y	148	40.2	3.681	0.520
At middle of third strip	at 0.2 Y	160	40.4	3.960	0.557
	at 0.6 Y	158	40.4	3.910	0.550
	at 0.8 Y	158	40.4	3.910	0.550

Run 10:

Geobag(Yellow),B1,Date=16/12/17 Initial water flow (Discharge)= 150 m3/h

Initial depth of flow= 0.25m
Flume Width = 0.762m
Total Depth of Flow Y=0.43 m
Current meter constant, a= 0.1334

Final water flow (Discharge)= 705 m3/h
Width of each strip, B/3 = 0.254 m
b= 0.029

Location of Current meter		Current meter reading			Point Velocity V (m/s)
Horizontal	Vertical	Number of revolution N (rev).	Time of observation T (sec)	Revolution per second n (rev/see)	
At middle of first strip	at 0.2 Y	178	40.5	4.395	0.615
	at 0.6 Y	173	40.4	4.282	0.600
	at 0.8 Y	164	40.4	4.059	0.570
At middle of Second strip	at 0.2 Y	184	40.5	4.543	0.635
	at 0.6 Y	188	40.6	4.630	0.646
	at 0.8 Y	180	40.2	4.477	0.6263
At middle of third strip	at 0.2 Y	185	40	4.625	0.645
	at 0.6 Y	185	40.3	4.590	0.641
	at 0.8 Y	182	40.1	4.538	0.634

Run 11:

Geobag (Blue)

B2,

Date=16/12/17, (discharge)= 150 m3/h Width of each strip, B/3 = 0.254 m

Initial depth of flow= 0.25m Final water flow (Discharge)= 665 m3/h

Current meter constant, a= 0.1334

Location of Current meter		Current meter reading			Point Velocity V (m/s)
Horizontal	Vertical	Number of revolution N (rev).	Time of observation T (sec)	Revolution per second n (rev/see)	
At middle of first strip	at 0.2 Y	181	40.4	4.480	0.626
	at 0.6 Y	175	40.4	4.331	0.606
	at 0.8 Y	158	40.3	3.920	0.552
At middle of Second strip	at 0.2 Y	181	40.2	4.502	0.629
	at 0.6 Y	182	40.4	4.504	0.629
	at 0.8 Y	176	40.2	4.378	0.613
At middle of third strip	at 0.2 Y	183	40.3	4.540	0.634
	at 0.6 Y	183	40.2	4.552	0.636
	at 0.8 Y	179	40.2	4.452	0.622

Run 12:

Geobag, Yellow, B1, Date=05/01/18

Initial water flow (Discharge)= 150 m3/h

Initial depth of flow= 0.30m — Final water flow (Discharge)= 790 m3/h

Flume Width = 0.762m — Width of each strip, B/3 = 0.254 m

Total Depth of Flow Y=0. 45m — b= 0.029

Current meter constant, a= 0.1334

Location of Current meter		Current meter reading			Point Velocity V (m/s)
Horizontal	Vertical	Number of revolution N (rev).	Time of observation T (sec)	Revolution per second n (rev/see)	
At middle of first strip	at 0.2 Y	177	40.3	4.392	0.614
	at 0.6 Y	175	39.9	4.385	0.614
	at 0.8 Y	167	40.3	4.143	0.581
At middle of Second strip	at 0.2 Y	182	40.4	4.504	0.629
	at 0.6 Y	182	40.4	4.504	0.629
	at 0.8 Y	176	40.2	4.378	0.613
At middle of third strip	at 0.2 Y	180	40.4	4.455	0.623
	at 0.6 Y	181	40.2	4.502	0.629
	at 0.8 Y	174	39.9	4.360	0.610

Run 13:

Geobag (White)A1,

Date=26/03/18 Initial water flow (Discharge)= 150 m3/h

Initial depth of flow= 0.25m Final water flow (Discharge)= 605 m3/h

Flume Width = 0.762r Width of each strip, B/3 = 0.254 m

Total Depth of Flow Y=0.37 m b= 0.029

Current meter constant, a= 0.1334

Location of Current meter		Current meter reading			Point Velocity V (m/s)
Horizontal	Vertical	Number of revolution N (rev).	Time of observation T (sec)	Revolution per second n (rev/see)	
At middle of first strip	at 0.2 Y	187	40.5	4.617	0.644
	at 0.6 Y	184	40.4	4.554	0.636
	at 0.8 Y	163	40.4	4.034	0.567
At middle of Second strip	at 0.2 Y	190	40.3	4.714	0.657
	at 0.6 Y	191	40.3	4.739	0.661
	at 0.8 Y	182	40.3	4.516	0.631
At middle of third strip	at 0.2 Y	193	40.5	4.765	0.664
	at 0.6 Y	195	40.9	4.767	0.665
	at 0.8 Y	183	40.3	4.540	0.634

Run 14:

Geobag (White)A1, Date=26/03/18 Initial water flow (Discharge)= 150 m3/h
Initial depth of flow= 0.30m Final water flow (Discharge)= 665 m3/h
Flume Width = 0.762 Width of each strip, B/3 = 0.254 m
Total Depth of Flow Y=0.43 m b= 0.029
Current meter constant, a= 0.1334

Location of Current meter		Current meter reading			Point Velocity V (m/s)
Horizontal	Vertical	Number of revolution N (rev).	Time of observation T (sec)	Revolution per second n (rev/see)	
At middle of first strip	at 0.2 Y	167	40.4	4.133	0.580
	at 0.6 Y	159	40.4	3.935	0.554
	at 0.8 Y	141	40.4	3.490	0.494
At middle of Second strip	at 0.2 Y	174	40.6	4.285	0.600
	at 0.6 Y	169	40.3	4.193	0.588
	at 0.8 Y	162	40.4	4.009	0.563
At middle of third strip	at 0.2 Y	173	40.3	4.292	0.601
	at 0.6 Y	174	40.5	4.296	0.602
	at 0.8 Y	171	40.5	4.222	0.592

Run 15:

Geobag (While)A2, Date= 26/03/18
Initial depth of flow= 0.30m
Flume Width = 0.762m
Total Depth of Flow Y=0.435 m
Current meter constant, a= 0.1334

Initial water flow (Discharge)= 150 m3/h
Final water flow (Discharge)= 690 m3/h
Width of each strip, B/3 = 0.254 m
b= 0.029

Location of Current meter		Current meter reading			Point Velocity V (m/s)
Horizontal	Vertical	Number of revolution N (rev).	Time of observation T (sec)	Revolution per second n (rev/see)	
At middle of first strip	at 0.2 Y	175	40.6	4.310	0.604
	at 0.6 Y	162	40.5	4	0.562
	at 0.8 Y	151	40.6	3.719	0.525
At middle of Second strip	at 0.2 Y	178	40.4	4.405	0.616
	at 0.6 Y	177	40.6	4.359	0.610
	at 0.8 Y	171	40.4	4.232	0.593
At middle of third strip	at 0.2 Y	171	39.4	4.340	0.607
	at 0.6 Y	176	40.5	4.345	0.608
	at 0.8 Y	173	40.7	4.250	0.596

Run 16:

Geobag (White) A2, Date=01/04/18

Initial water flow (Discharge)= 150 m3/h

Initial depth of flow= 0.25m — Final water flow (Discharge)= 511 m3/h

Flume Width = 0.762r — Width of each strip, B/3 = 0.254 m

Total Depth of Flow Y=0.35 m — b= 0.029

Current meter constant, a= 0.1334

Location of Current meter		Current meter reading			Point Velocity V (m/s)
Horizontal	Vertical	Number of revolution N (rev).	Time of observation T (sec)	Revolution per second n (rev/see)	
At middle of first strip	at 0.2 Y	162	40.8	3.970	0.558
	at 0.6 Y	157	40.2	3.905	0.549
	at 0.8 Y	151	40.6	3.719	0.525
At middle of Second strip	at 0.2 Y	168	40.6	4.137	0.581
	at 0.6 Y	168	40.7	4.127	0.579
	at 0.8 Y	156	40.2	3.880	0.546
At middle of third strip	at 0.2 Y	167	40.4	4.133	0.580
	at 0.6 Y	169	40.7	4.152	0.582
	at 0.8 Y	160	40.4	3.960	0.557

Run 17:

Geobag C
Initial depth of flow= 0.30m
Flume Width = 0.762m
Total Depth of Flow Y=0.425 m
Current meter constant, a= 0.1334

Initial water flow (Discharge)= 150 m3/h
Final water flow (Discharge)= 655 m3/h
Width of each strip, B/3 = 0.254 m
b= 0.029

Location of Current meter		Current meter reading			Point Velocity V (m/s)
Horizontal	Vertical	Number of revolution N (rev).	Time of observation T (sec)	Revolution per second n (rev/see)	
At middle of first strip	at 0.2 Y	156	40.4	3.861	0.544
	at 0.6 Y	148	40.2	3.681	0.520
	at 0.8 Y	137	40.4	3.391	0.481
At middle of Second strip	at 0.2 Y	163	40.4	4.0346	0.567
	at 0.6 Y	160	40.4	3.960	0.557
	at 0.8 Y	160	40.7	3.931	0.553
At middle of third strip	at 0.2 Y	160	40.3	3.970	0.558
	at 0.6 Y	161	40.4	3.985	0.560
	at 0.8 Y	160	40.3	3.970	0.558

Run 18:

Geobag C
Initial depth of flow= 0.25m
Flume Width = 0.762m
Total Depth of Flow Y=0. 365m
Current meter constant, a= 0.1334

Initial water flow (Discharge)= 150 m3/h
Final water flow (Discharge)= 620 m3/h
Width of each strip, B/3 = 0.254 m
b= 0.029

Location of Current meter		Current meter reading			Point Velocity V (m/s)
Horizontal	Vertical	Number of revolution N (rev).	Time of observation T (sec)	Revolution per second n (rev/see)	
At middle of first strip	at 0.2 Y	188	40	4.7	0.655
	at 0.6 Y	174	39.4	4.416	0.618
	at 0.8 Y	168	40.3	4.168	0.618
At middle of Second strip	at 0.2 Y	188	40.1	4.688	0.654
	at 0.6 Y	191	40.2	4.751	0.662
	at 0.8 Y	183	40.5	4.518	0.631
At middle of third strip	at 0.2 Y	194	40.3	4.813	0.671
	at 0.6 Y	194	39.9	4.862	0.677
	at 0.8 Y	188	40.9	4.596	0.642